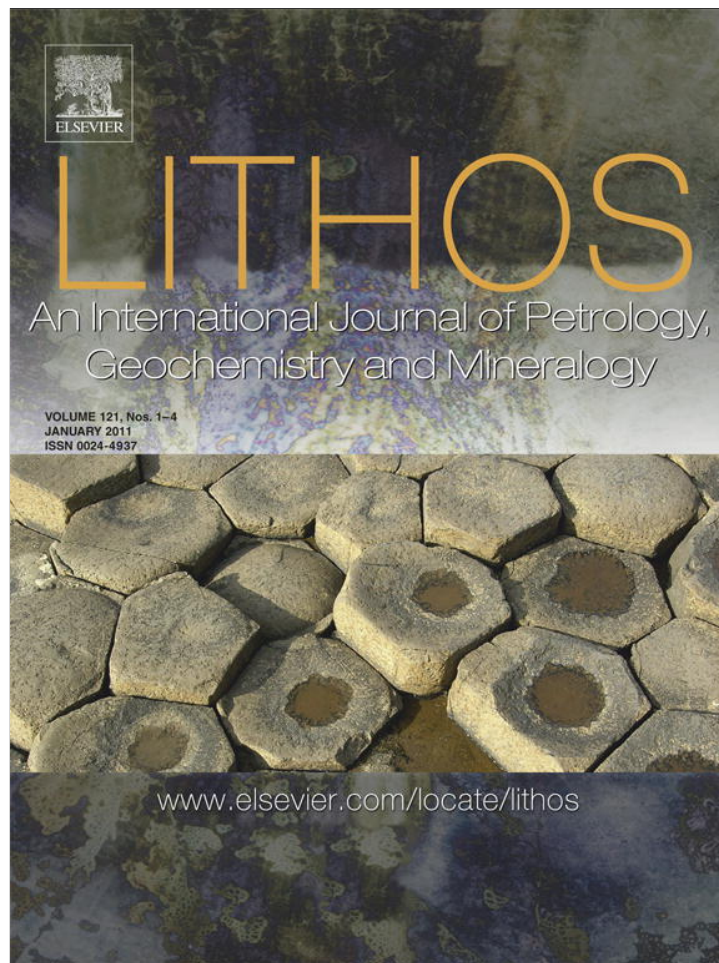


Provided for non-commercial research and education use.
Not for reproduction, distribution or commercial use.



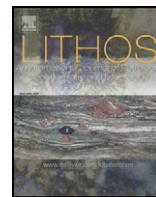
(This is a sample cover image for this issue. The actual cover is not yet available at this time.)

This article appeared in a journal published by Elsevier. The attached copy is furnished to the author for internal non-commercial research and education use, including for instruction at the authors institution and sharing with colleagues.

Other uses, including reproduction and distribution, or selling or licensing copies, or posting to personal, institutional or third party websites are prohibited.

In most cases authors are permitted to post their version of the article (e.g. in Word or Tex form) to their personal website or institutional repository. Authors requiring further information regarding Elsevier's archiving and manuscript policies are encouraged to visit:

<http://www.elsevier.com/copyright>



Petrology of the Mesoarchean Rio Maria suite and the discrimination of sanukitoid series

Marcelo Augusto de Oliveira ^{a,b,*}, Roberto Dall'Agnol ^a, José de Arimatéia Costa de Almeida ^{a,b}

^a Group of Research on Granite Petrology, Instituto de Geociências (IG), Universidade Federal do Pará (UFPA), Caixa Postal 8608, 66075-900 Belém, Pará, Brazil

^b Faculdade de Geologia do Campus de Marabá, UFPA, Brazil

ARTICLE INFO

Article history:

Received 10 June 2011

Accepted 28 August 2011

Available online 5 September 2011

Keywords:

Amazonian craton

High-Mg granitoids

Sanukitoids

Petrogenesis

Modeling

Metasomatized mantle

ABSTRACT

The rocks of 2.87 Ga Rio Maria sanukitoid suite of the eastern Amazonian craton include granodiorites, intermediate rocks, layered rocks and mafic enclaves. Their REE patterns and the behavior of Rb, Ba, Sr, and Y allowed the distinction of a granodioritic (granodiorite and intermediate rocks) and a monzonitic (mafic enclaves) sanukitoid series. Petrogenetic modeling indicated that the granodiorites and intermediate rocks are not related by fractional crystallization. The internal evolution of the intermediate rocks were led by fractionation of amphibole + biotite ± apatite, whereas the granodiorites evolved by fractionation of plagioclase + amphibole ± biotite. The layered rocks were probably derived from the granodiorite magma by an accumulation of 50% of amphibole (dark layer) and of 30% of amphibole ± plagioclase (gray layer). The petrogenesis of the Rio Maria suite required melting of a modified mantle extensively metasomatized by addition of about 30% TTG-like melt to generate the granodiorite (11% of melt) and intermediate magmas (14% of melt), and ~20% TTG-like melt in the case of mafic enclave magma (9% of melt).

Modeling and geochemical data, particularly the behavior of Sr and Y, suggest that mafic enclave and granodiorite magmas were originated at different depths and should have mingled during their ascent and final emplacement. The modal and geochemical differences observed between the granodioritic and monzonitic sanukitoid series of Rio Maria are apparently a general feature of the Archean sanukitoids. This indicates the existence of at least two distinct sanukitoid series and suggests that the nature of the sanukitoid series is strongly dependent of the pressure of magma generation.

Our results indicate that the sanukitoid magmas were originated in a two stage process. The envisaged model admits an active subduction tectonic setting in the Rio Maria terrane in between 2.98 and 2.92 Ga when the TTG magmas responsible by the mantle metasomatism were generated (first stage). At ~2.87 Ga, a tectonothermal event, possibly related to slab-break-off or due to the action of a mantle plume, induced the partial melting of the metasomatized mantle and generated the Rio Maria sanukitoid magmas (second stage).

Published by Elsevier B.V.

1. Introduction

In several cratons, Meso to Late Archean evolution (<3.0 Ga) was characterized by intense magmatic activity. The TTG suites are the more voluminous rocks formed in Archean terranes, but the relevance of high-Mg granitoids (sanukitoids) was also demonstrated (Stern et al., 1989; Moyen et al., 2003; Smithies et al., 2004; Halla, 2005; Heilimo et al., 2010). Sanukitoid rocks display geochemical characteristics similar to both mantle- and crust-derived magmatic rocks and were identified in various Archean terranes (cf. Heilimo et al., 2011 and references therein). Independent of the processes

responsible for their origin, it is widely accepted that TTG series derived from partial melting of hydrated metabasalts (Martin, 1994, 1999; Bédard et al., 2003; Smithies et al., 2004; Condie, 2005; Martin et al., 2005). On the other hand, the role of TTG magmas in the origin of sanukitoid suites remains controversial and the petrogenesis of the latter is not well constrained.

To explain the origin of sanukitoid magmas several processes have been tested. Stern et al. (1989) modeled contamination of basaltic or komatiitic magmas by a LILE-rich felsic crust. They concluded that the interaction between mafic or ultramafic melts and crustal material could not have produced the compositions of primitive sanukitoids. However, Pb isotopic data indicate a significant crustal influence in sanukitoid magma evolution and their generally high Ba and Sr contents were attributed to recycling of sedimentary rocks associated with the slab (Halla, 2005). Additionally, partial melting of mantle peridotite that had been previously metasomatized by TTG melts (Evans and Hanson, 1997; Smithies and Champion, 2000) or slab-melts

* Corresponding author at: Group of Research on Granite Petrology, Instituto de Geociências (IG), Universidade Federal do Pará (UFPA), Caixa Postal 8608, 66075-900 Belém, Pará, Brazil. Tel.: + 55 91 3201 7477.

E-mail addresses: mao@ufpa.br (M.A. Oliveira), robdal@ufpa.br (R. Dall'Agnol), ari@ufpa.br (J.A.C. Almeida).

that had assimilated peridotite during ascent through mantle wedge (Martin et al., 2005; Rapp et al., 2010), offer an alternative explanation for the petrogenesis of these rocks (Rapp et al., 1999, 2007, 2010). Another hypothesis advocates that fluids liberated by slab

dehydration processes would be responsible for the mantle metasomatism (Halla, 2005).

Smithies and Champion (2000) showed that sanukitoids are late- to post-kinematic intrusions (Stern et al., 1989; Evans and Hanson,

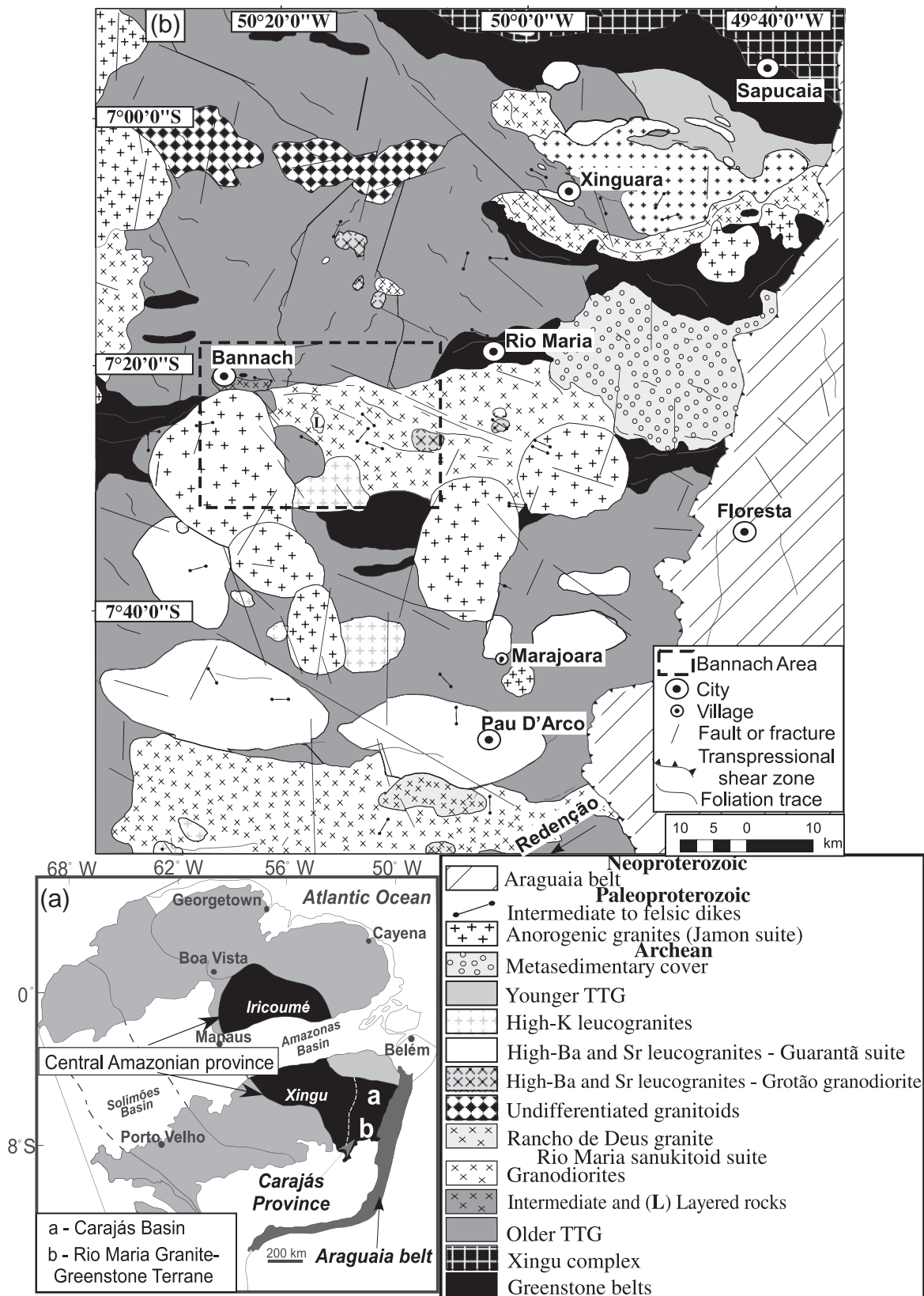


Fig. 1. (a) Location of the studied area in the Amazonian craton; (b) Geological map of the Rio Maria granite-greenstone terrane (modified from Leite, 2001).

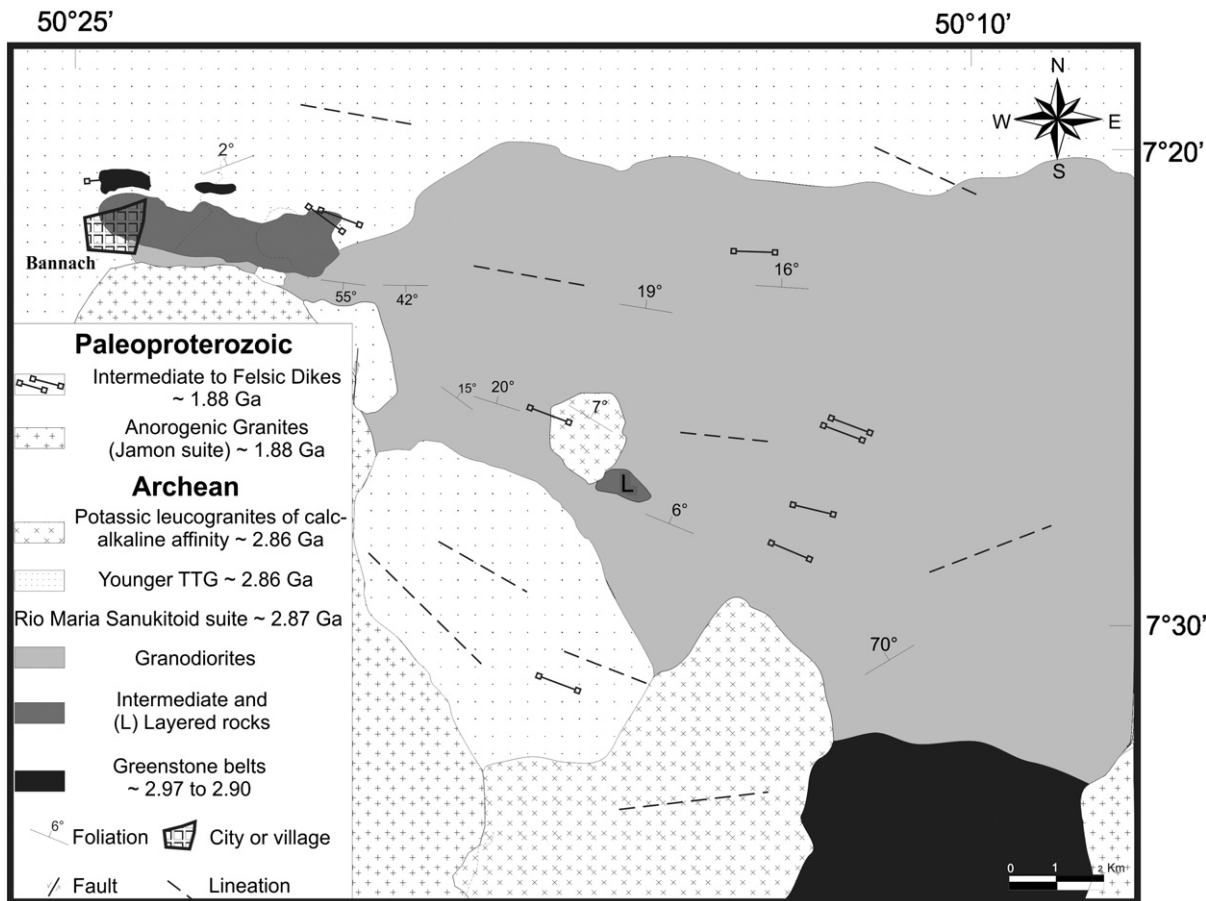


Fig. 2. Geological map of Bannach area (Oliveira et al., 2006).

1997), which are in general not temporally associated with the TTG magmas (Lobach-Zhuchenko et al., 2005; Heilimo et al., 2011). High-Mg suites are the only Archean granitoid series that appears to be derived from the mantle (Moyen, 2011), and an understanding of its petrogenesis, tectonic setting and possible relationship to the TTG series may clarify the processes involved in the Archean crustal evolution.

Typical sanukitoid rocks have been identified in the Rio Maria granite–greenstone terrane, southeast of the Amazonian craton and form the ~2.87 Ga old Rio Maria suite (Althoff et al., 2000; Oliveira

et al., 2009, 2010). These rocks are post-kinematic intrusions into 2.98 to 2.90 Ga supracrustal sequences and TTG suites. This paper presents extensive geochemical data on the sanukitoid rocks from the Bannach area representative of the Rio Maria suite. The aim of this paper is to explore geochemical data with modeling techniques to discuss the contrasts between granodioritic and monzonitic sanukitoid series, the sources and evolution of the sanukitoid magmas, and to contribute to clarifying the role of convergent plate margin processes and mantle metasomatism in the origin of sanukitoid series.

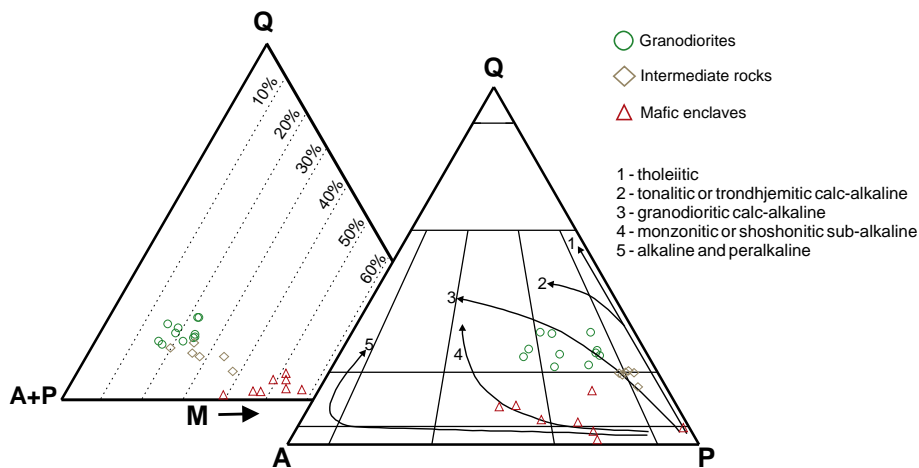


Fig. 3. QAP and Q-(A+P)-M plots for the rocks of the Rio Maria suite. Data sources: Granodiorites and intermediate rocks (Oliveira, 2005); Mafic enclaves (Oliveira et al., 2010).

Table 1
Chemical composition of the rocks of the Rio Maria suite (Bannach area).

Facies	Layered rocks						Mafic enclaves							
	Dark layer			Gray later			EBAD to EBAQMz							
Sample	MFR-07B	MFR-12B	ADR-1	MFR-	CR-71	MFR-12A	MFR-27C	MD-02C	MD-03A	299	MD-02A	ADR-2	MD-02B	MD-03B
SiO ₂ (wt.%)	50.92	52.60	54.04	50.14	52.60	53.41	50.51	51.38	52.89	53.03	53.3	54.98	55.46	56.64
TiO ₂	0.73	0.56	0.63	0.97	0.70	0.78	0.88	0.72	0.69	0.72	0.69	0.61	0.55	0.85
Al ₂ O ₃	12.11	10.91	13.02	13.08	13.21	14.76	16.19	13.77	15.63	13.56	12.29	14.34	13.09	13.28
Fe ₂ O ₃	4.16	3.28	3.41	3.63	11.89	4.07	5.06	11.15	9.58	10.49	10.2	3.59	8.94	9.05
FeO	5.96	5.96	3.41	7.08	n.d.	4.83	4.46	n.d.	n.d.	n.d.	n.d.	4.14	n.d.	n.d.
MnO	0.15	0.15	0.13	0.15	0.15	0.13	0.13	0.2	0.17	0.18	0.19	0.14	0.17	0.16
MgO	9.94	10.51	7.37	8.48	9.17	5.98	5.65	7.38	6.28	8.39	7.43	5.82	6.61	6.61
CaO	8.21	9.3	8.15	8.81	8.55	7.88	7.61	8.36	7.66	7.79	7.42	6.73	6.24	6.52
Na ₂ O	2.49	2.06	2.86	2.60	2.36	2.99	4.06	3.53	4.72	2.87	2.31	3.86	2.59	3.83
K ₂ O	2.04	1.03	1.74	1.72	1.94	2.00	2.33	1.94	1.1	2.32	4.23	3.07	4.96	1.76
P ₂ O ₅	0.22	0.15	0.17	0.17	0.24	0.23	0.45	0.37	0.33	0.25	0.31	0.27	0.29	0.31
LOI	2.10	2.50	2.30	2.00	n.d.	2.10	1.90	0.80	0.60	n.d.	1.20	1.60	0.60	0.60
Total	99.03	99.01	99.10	98.83	100.81	99.16	99.23	99.56	99.65	99.60	99.57	99.15	99.50	99.61
Ba(ppm)	511	442	527	608	n.d.	711	344	468	199	1145	1088	876	1382	417
Rb	118	39	80	77	115	84	140	89	56	98	125	94	101	77
Sr	477	335	507	494	422	604	800	508	544.8	445	357.7	463	338	436
Zr	97	81	92	87	116	99	165	140	151	129	118	105	103	153
Nb	5	4	5	5	5	5	7	8	7	11	11	11	7	7
Y	17	17	17	23	15	19	23	23	22	24	25	23	19	23
Ga	17	14	17	18	n.d.	20	25	19	20	n.d.	16	20	15	17
Th	8	6	6	6	n.d.	6	1	2	2	n.d.	2	5	2	3
Ni	105	61	80	82	n.d.	57	46	40	18	n.d.	40	47	40	52
Cr	253	417	239	212	n.d.	171	103	397	226	n.d.	506	281	465	335
La	33	24.3	25.4	31.8	n.d.	27.6	28.5	25.00	25.4	n.d.	22.4	29	18.4	30.8
Ce	62.8	43.7	55.2	67.2	n.d.	53.9	77.1	67.2	60.4	n.d.	64.8	72.1	50.2	71.00
Pr	6.47	5.28	5.69	6.97	n.d.	6.54	10.11	10.41	9.85	n.d.	10.43	9.42	7.99	10.41
Nd	25.1	20.9	24.5	28.9	n.d.	27.1	44	41.6	43.5	n.d.	43.00	40.4	32.8	41.8
Sm	4.80	4.10	4.50	6.10	n.d.	5.30	8.60	8.40	8.35	n.d.	8.61	7.50	6.62	7.91
Eu	1.29	1.14	1.33	1.69	n.d.	1.59	1.73	1.58	1.62	n.d.	1.75	1.52	1.27	1.59
Gd	4.04	3.59	3.64	5.06	n.d.	4.74	5.71	6.65	6.64	n.d.	6.92	5.8	5.4	6.7
Tb	0.60	0.51	0.58	0.82	n.d.	0.72	0.86	0.97	0.88	n.d.	0.96	0.98	0.74	0.88
Dy	2.82	2.79	2.89	3.90	n.d.	3.37	4.35	4.94	4.36	n.d.	4.66	4.00	3.83	4.50
Ho	0.54	0.53	0.6	0.77	n.d.	0.69	0.78	0.87	0.81	n.d.	0.87	0.74	0.71	0.8
Er	1.51	1.52	1.68	2.14	n.d.	1.82	2.05	2.41	2.14	n.d.	2.33	2.04	1.88	2.16
Tm	0.23	0.24	0.19	0.33	n.d.	0.26	0.29	0.37	0.32	n.d.	0.38	0.27	0.28	0.35
Yb	1.55	1.36	1.41	1.8	n.d.	1.48	1.7	2.24	1.85	n.d.	2.3	1.73	1.69	1.88
Lu	0.22	0.2	0.23	0.3	n.d.	0.25	0.25	0.32	0.28	n.d.	0.34	0.29	0.26	0.28
ΣREE	144.97	110.16	127.84	157.78	n.d.	135.36	186.03	172.96	166.4	n.d.	169.75	175.7	132.07	181.06
(La/Yb) _n	14.37	12.06	12.16	11.92	n.d.	12.59	11.32	7.53	9.27	n.d.	6.57	11.31	7.35	11.06
(La/Sm) _n	4.33	3.73	3.55	3.28	n.d.	3.28	2.09	1.87	1.92	n.d.	1.64	2.43	1.75	2.45
(Dy/Yb) _n	1.18	1.33	1.33	1.41	n.d.	1.48	1.66	1.43	1.53	n.d.	1.32	1.5	1.47	1.56
Eu/Eu*	0.9	0.91	1.0	0.93	n.d.	0.97	0.75	0.65	0.67	n.d.	0.69	0.7	0.65	0.67
Rb/Sr	0.25	0.12	0.16	0.16	0.27	0.14	0.17	0.18	0.10	0.22	0.35	0.20	0.30	0.18
Sr/Ba	0.93	0.76	0.96	0.81	n.d.	0.85	2.32	1.09	2.74	0.39	0.33	0.53	0.24	1.04
K/Na	0.54	0.33	0.40	0.44	0.54	0.44	0.38	0.36	0.15	0.53	1.20	0.52	1.26	0.30
FeO _t /(FeO _t + MgO)	0.49	0.46	0.47	0.55	0.54	0.59	0.61	0.58	0.58	0.53	0.55	0.56	0.55	0.55
Mg#	0.64	0.67	0.61	0.59	0.60	0.55	0.55	0.56	0.56	0.61	0.59	0.58	0.59	0.59

Data source: Oliveira (2005). Chemical ratios: Mg# molecular ratio Mg/(Mg + Fe); K/Na molecular ratio. Eu/Eu* = EuN/(0.5 (SmN + GdN)). E = epidote; B = biotite; A = amphibole; Qz = quartz; D = diorite; MzD = monzodiorite; Mz = monzonite; GD = granodiorite; MzG = monzogranite.

2. Geologic setting

The Rio Maria sanukitoid suite is exposed in the Carajás province of the eastern Amazonian craton (Machado et al., 1991; Macambira and Lafon, 1995; Rämö et al., 2002; Dall'Agnol et al., 2006). The Carajás province comprises mostly Archean rocks intruded by Paleoproterozoic anorogenic granites (Dall'Agnol et al., 2005).

The Carajás province is divided into the Rio Maria granite–greenstone terrane (3.0 to 2.86 Ga; Macambira and Lafon, 1995; Dall'Agnol et al., 2006, 2011), and the Carajás domain (3.0 to 2.55 Ga; Machado et al., 1991; Macambira and Lafon, 1995; Barros et al., 2001). The Rio Maria granite–greenstone terrane (RMGGT; Fig. 1b) consists of greenstone belts and Archean granitoids partially covered by sediments of the Rio Fresco group.

In the RMGGT, the greenstone-belts (Andorinhas supergroup) are composed mostly of komatiites and tholeiitic basalts (2.98–2.90 Ga;

Huhn et al., 1988; Souza et al., 2001). The Archean granitoids have ages between 2.98 and 2.86 Ga and five principal groups have been distinguished (Dall'Agnol et al., 2011): (1) An older tonalitic–trondhjemitic series (TTG) represented by the Arco Verde, Caracol and Mariazinha tonalites and the Mogno trondhjemitic (~2.98 to 2.92 Ga; Althoff et al., 2000; Leite et al., 2004; Guimarães et al., 2010; Almeida et al., 2011); (2) The 2.87 Ga Rio Maria sanukitoid suite formed by the different occurrences of the Rio Maria granodiorite and associated rocks (Medeiros, 1987; Macambira and Lancelot, 1996; Althoff et al., 2000; Leite et al., 2004; Oliveira et al., 2009, 2010); (3) A 2.87 Ga leucogranodiorite–leucogranite group (Guarantã suite and similar rocks; Almeida et al., 2010); (4) A younger TTG series represented by the Água Fria trondhjemitic (2.86 Ga; Leite et al., 2004; Almeida et al., 2011); and (5) 2.87 to 2.86 Ga Xinguara and Mata Surrão calc-alkaline potassic leucogranites (Lafon et al., 1994; Leite et al., 2004; Almeida et al., 2010). The last shearing deformational event occurred

Facies	Intermediate rocks						Granodiorites							
	EBAQzD to EBAQzMD						EBAGD to EBAMzG							
Sample	ADR-4A	ADR-4B	ADR-5	MFR-102	MFR-100D	ADR-7	MFR-114	MFR-27	MFR-111	MFR-29	ADR-3A	MFR-112	MFR-91A	MFR-80A
SiO ₂ (wt.%)	58.47	60.51	61.75	62.15	63.29	63.61	62.52	63.23	63.66	63.66	63.9	64.58	64.72	66.49
TiO ₂	0.47	0.44	0.43	0.39	0.38	0.37	0.46	0.49	0.42	0.45	0.43	0.42	0.39	0.33
Al ₂ O ₃	14.02	14.03	13.96	14.5	14.97	14.94	15.23	14.82	14.87	14.84	14.82	14.65	14.98	14.55
Fe ₂ O ₃	2.46	2.37	2.89	2.34	2.51	3.12	2.91	2.8	2.81	3.00	2.91	2.86	2.71	2.27
FeO	3.94	3.43	2.44	2.56	1.96	1.41	1.97	1.89	1.64	1.48	1.65	1.47	1.49	1.32
MnO	0.09	0.09	0.07	0.07	0.06	0.06	0.07	0.06	0.06	0.06	0.06	0.06	0.06	0.05
MgO	5.81	5.37	4.62	4.11	2.89	2.86	2.61	2.49	2.31	2.31	2.39	2.28	2.06	1.85
CaO	5.88	4.73	4.84	4.65	4.18	4.03	4.4	4.36	3.99	4.17	4.02	3.77	4.08	3.02
Na ₂ O	3.77	4.04	3.98	4.21	4.36	4.4	4.3	4.21	4.19	4.09	4.05	4.04	4.29	4.13
K ₂ O	2.21	2.16	2.31	2.24	2.57	2.66	2.93	3.01	3.32	3.22	3.21	3.44	2.98	3.75
P ₂ O ₅	0.17	0.18	0.16	0.14	0.15	0.13	0.17	0.15	0.15	0.14	0.14	0.15	0.12	0.14
LOI	1.90	1.90	1.90	2.00	2.00	1.80	1.60	1.80	1.90	1.90	1.80	1.50	1.50	1.40
Total	99.19	99.25	99.35	99.36	99.32	99.39	99.17	99.31	99.32	99.32	99.38	99.22	99.38	99.30
Ba(ppm)	812	701	847	830	1008	1090	1139	1175	1052	1022	1098	1064	1044	1089
Rb	73	72	72	74	87	82	98	103	113	112	109	122	101	116
Sr	745	618	724	828	872	905	692	661	615	611	576	567	632	512
Zr	94	94	101	94	95	103	113	126	103	131	109	110	113	122
Nb	6	5	6	5	6	7	8	9	8	8	7	11	9	10
Y	11	10	11	10	10	12	16	13	11	15	11	12	17	12
Ga	18	18	19	20	20	20	20	20	19	20	20	19	20	19
Th	3	2	5	5	6	5	7	7	7	8	5	11	8	12
Ni	79	89	81	72	43	57	31	29	28	29	31	29	26	25
Cr	308	253	274	219	130	144	48	68	55	96	68	55	41	55
La	23.7	23.3	25.1	25.2	42.2	33.8	37.3	36.9	33.7	34.3	20.0	40.7	53.5	48.0
Ce	51.1	50.3	51.4	47.6	68.3	58.6	72.8	71.9	64.1	64.1	45.7	70.8	72.2	64.2
Pr	5.35	5.35	5.3	5.35	7.37	7.35	7.19	7.57	6.32	6.53	4.94	7.04	8.51	6.81
Nd	21.4	21.4	19.3	20.8	26.1	29.2	27.2	27.8	22.9	24.7	21.7	25.6	31.6	23.9
Sm	3.60	3.40	3.30	3.60	4.10	4.30	4.40	4.90	3.70	4.30	3.70	3.90	4.50	3.40
Eu	1.02	0.95	0.98	0.99	1.05	1.23	1.25	1.35	1.06	1.14	1.05	1.07	1.30	0.95
Gd	2.78	2.49	2.58	2.42	2.82	3.19	3.47	3.56	2.9	3.2	2.63	2.71	3.37	2.43
Tb	0.45	0.37	0.37	0.4	0.35	0.48	0.56	0.53	0.42	0.47	0.41	0.40	0.52	0.36
Dy	2.25	1.84	1.98	1.75	1.67	2.20	2.41	2.19	1.92	2.19	1.86	1.90	2.31	1.56
Ho	0.38	0.34	0.33	0.34	0.31	0.42	0.48	0.42	0.34	0.42	0.41	0.4	0.49	0.32
Er	1.03	0.97	0.88	0.95	0.78	1.13	1.3	1.15	0.92	1.19	1.02	0.92	1.25	0.81
Tm	0.13	0.1	0.1	0.1	0.11	0.13	0.14	0.17	0.11	0.17	0.1	0.23	0.17	0.12
Yb	0.93	0.83	0.81	0.9	0.69	1.00	1.00	1.06	0.92	1.09	0.87	0.83	0.99	0.73
Lu	0.15	0.14	0.12	0.13	0.12	0.15	0.16	0.16	0.11	0.15	0.14	0.15	0.15	0.13
ΣREE	114.27	111.78	112.55	110.53	155.97	143.18	159.66	159.66	139.42	143.95	104.53	156.65	180.86	153.72
(La/Yb) _n	17.20	18.95	20.92	18.90	41.28	22.81	25.18	23.50	24.72	21.24	15.52	33.10	36.48	44.38
(La/Sm) _n	4.14	4.31	4.79	4.41	6.48	4.95	5.34	4.74	5.73	5.02	3.40	6.57	7.49	8.89
(Dy/Yb) _n	1.57	1.44	1.59	1.26	1.57	1.43	1.57	1.34	1.36	1.31	1.39	1.49	1.52	1.39
Eu/Eu*	0.99	1.00	1.03	1.03	0.94	1.02	0.98	0.99	0.99	0.94	1.03	1.01	1.02	1.01
Rb/Sr	0.1	0.12	0.1	0.09	0.1	0.09	0.14	0.16	0.18	0.18	0.19	0.22	0.16	0.23
Sr/Ba	0.92	0.88	0.85	1.00	0.86	0.83	0.61	0.56	0.58	0.6	0.53	0.53	0.61	0.47
K/Na	0.39	0.35	0.38	0.35	0.39	0.40	0.45	0.47	0.52	0.52	0.52	0.56	0.46	0.60
FeOt/(FeOt + MgO)	0.52	0.51	0.52	0.53	0.59	0.60	0.64	0.64	0.64	0.64	0.64	0.64	0.66	0.65
Mg#	0.62	0.63	0.62	0.61	0.55	0.54	0.50	0.50	0.50	0.49	0.49	0.50	0.48	0.49

at around 2.87 Ga (Althoff et al., 2000; Souza et al., 2001; Leite, 2001) and, subsequently, the RMGGT remained stable until the emplacement of 1.88 Ga A-type granites.

3. Geologic and geochronologic aspects

The Bannach area was selected for this study because it contains the largest expositions of mafic and intermediate rocks associated and cogenetic with the Rio Maria granodiorite (Oliveira et al., 2009). In the Bannach area, the dominant variety of rock is an epidote–biotite–hornblende granodiorite and the associated intermediate and mafic rocks occur in two domains. Near Bannach, it is exposed a stock composed mostly of quartz diorites and quartz monzodiorites and along the road between Rio Maria and Bannach, there is an occurrence of layered rocks (Fig. 2). More detailed information about these

rocks, as well as about the mafic enclaves and their relationships with host granodiorites, is provided by Oliveira et al. (2009, 2010).

Zircon dating by the Pb–evaporation method (Kober, 1986) was accomplished at the Laboratório de Geologia Isotópica (Pará-Iso) of the Universidade Federal do Pará, Belém. Analytical methods were described by Gaudette et al. (1998) and are available in the Supplemental data.

Representative samples of the Rio Maria granodiorite from different areas of the RMGGT yielded remarkably uniform U–Pb and Pb–Pb evaporation zircon ages (~2.87 Ga; Supplemental data Table A1). Two intermediate sanukitoid rocks dated by the single zircon Pb–evaporation method gave ages of 2878 ± 4 Ma (a restrict occurrence near Xinguara; Dall'Agnol et al., 1999) and 2875 ± 2 Ma (Parazonia quartz diorite; Guimarães et al., in press). In the present work, zircons from an epidote–biotite–hornblende quartz diorite of Bannach (sample MFR-102; Oliveira et al., 2009) were dated by the Pb–

evaporation method (Fig. 2). Zircons are generally prismatic, yellowish, and translucent and six analyzed grains (Supplemental data Table A2, Supplemental Fig. A1) indicated an age of 2860 ± 2 Ma (2σ ; MSWD = 0.99). This age is interpreted as the emplacement age of the intermediate rocks and indicates that these rocks are a little younger than the dominant granodiorites.

4. Petrography

The general petrographic aspects of the Rio Maria suite from the Bannach area have been discussed by Oliveira et al. (2009, 2010). All facies of the Rio Maria suite present a strongly saussuritized plagioclase and contain amphibole \pm biotite \pm magmatic epidote as their principal mafic minerals. M' values (the total modal content of mafic minerals as a percentage) vary between 10 and 25 in the granodiorites, 20 and 40 in the intermediate rocks, and are ≥ 40 in the mafic enclaves (Fig. 3). The accessory minerals are apatite, magnetite, titanite, allanite, and zircon, the latter being absent only in the layered rocks.

The epidote–biotite–hornblende granodiorite displays an equigranular, medium- or coarse-even-grained texture and the quartz diorites and quartz monzodiorites show equigranular, medium- to fine-grained texture. The mineral assemblages and textural relationships between different minerals are very similar in the different rock varieties despite their modal variations.

The mineralogy of the layered rocks is similar to that of the Rio Maria granodiorite and intermediate rocks. The textural variations are directly related to the different layers of the rock (dark and gray layers, reflecting variation in modal content of mafic phases). The cumulus material is formed by centimeter-sized euhedral pargasite to magnesium–hornblende crystals, whereas the intercumulus material is mainly composed of intensely saussuritized plagioclase, with subordinate quartz, amphibole, biotite, and epidote. The accessory minerals are allanite, titanite, magnetite, and apatite.

The mafic enclaves have dioritic to quartz monzonitic compositions (Oliveira et al., 2010) and follow a monzonitic trend in the QAP plot (Lameyre and Bowden, 1982), whereas the granodiorites and intermediate rocks follow a granodioritic trend. In the enclaves, the mineral assemblage is very similar to those found in the other rock varieties of the suite, but, considering their low modal contents of quartz, the enclaves have relatively higher modal alkali feldspar (Fig. 3). In the enclave samples, the presence of coarse poikilitical K-feldspar crystals including medium- to fine-grained euhedral amphibole is remarkable.

5. Geochemistry

5.1. General aspects

Chemical analyses of representative samples of the Rio Maria suite are given in Table 1. Major and trace elements were analyzed by ICP-ES and ICP-MS, respectively, at the Acme Analytical Laboratories Ltd. in Canada (Detection limits: 0.01 to 0.04 wt.% for major elements; 0.1 to 1.0 ppm for trace elements; 0.01 to 0.3 ppm for rare earth elements. Duplicate analyses of at least one sample were done systematically for each lot of samples).

The layered rocks, mafic enclaves, intermediate rocks, and granodiorites have in common a typical sanukitoid signature indicated by their metaluminous character, and high Mg#, Cr, and Ni, conjugate with elevated contents of large ion lithophile elements (LILE), especially Ba and Sr (Oliveira et al., 2009, 2010). Layered rocks and mafic enclaves have similar silica contents varying from 50.14 to 56.64 wt.% (Table 1), which illustrates a compositional gap between these rocks and the intermediate rocks and granodiorites (Fig. 4).

The alkali contents in the studied rocks are high compared to a typical calc-alkaline series. In the TAS diagram (Fig. 4; fields for

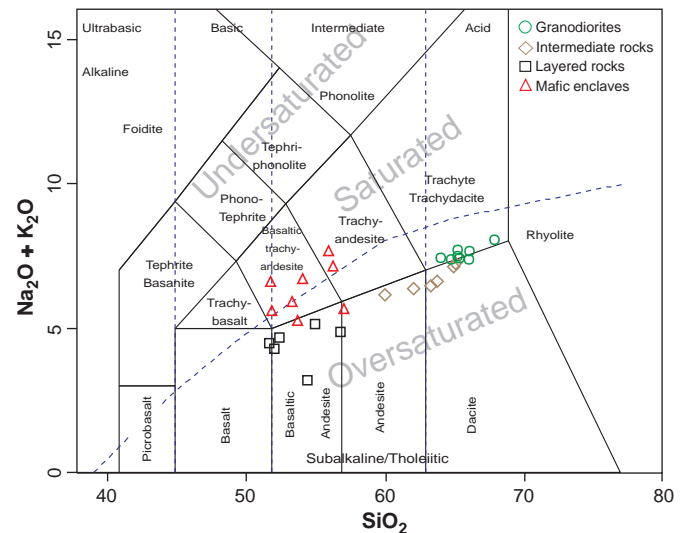


Fig. 4. The total alkali–silica diagram (TAS) showing the composition of rocks of the Rio Maria suite. TAS diagram classification according to Le Bas et al. (1986).

volcanic rocks of Le Maitre, 2002, are shown for comparison), the intermediate rocks and granodiorite samples plot along the divide between the oversaturated and saturated domains. On the other hand, the enclaves plot dominantly in the saturated field of that diagram, which is consistent with their affinity with the monzonitic series (Fig. 3). In the case of layered rocks, which were previously interpreted as cumulate rocks (Oliveira et al., 2010), it is clear that the analyzed samples do not correspond to real liquids and their chemical compositions are given for comparison.

Al_2O_3 contents (Table 1) are lower than those found in rocks of similar silica contents of typical calc-alkaline series (Irvine and Baragar, 1971; Ringwood, 1975; Wilson, 1989) and are similar in the enclaves, intermediate rocks and granodiorites, reaching the lowest values in the layered rocks. Mg# values vary from 0.67 to 0.48, decreasing from the layered rocks to the granodiorites (Table 1). The Mg# in the enclaves is generally intermediate between those of layered and intermediate rocks and granodiorites (Fig. 5c). K/Na ratios do not show accentuated variation in the different groups (Table 1), except for the quartz monzonitic enclaves which are enriched in K_2O compared to dominant rocks and display K/Na ratios of > 1 .

5.2. The behavior of trace elements

The trace elements are useful in estimating the extent of fractionation and whether magmatic evolution was dominated by fractional crystallization, partial melting or more complex processes (Hanson, 1978, 1989; Rämö, 1991; Rollinson, 1993; Dall'Agnol et al., 1999; Rapp et al., 1999; Smithies and Champion, 2000; Martin et al., 2005; Moyer, 2009).

5.2.1. Rb, Sr, and Ba

Rb behaves incompatibly in all varieties of the studied rocks (Table 1, Fig. 5a). In the granodiorites and mafic enclaves, the increase of Rb along magmatic differentiation is more accentuated than that in the intermediate rocks. Sr behavior contrasts in these rocks, as it is compatible in the granodiorites and mafic enclaves but incompatible in the intermediate rocks. Ba is clearly incompatible in the intermediate rocks and mafic enclaves and shows limited variation in the granodiorites. Rb and Sr show a positive correlation in the intermediate rocks, and a negative correlation in the granodiorites and mafic enclaves; Sr and Ba display a positive correlation in the intermediate rocks and a negative correlation in the mafic enclaves and granodiorites (Fig. 5a, b). In the Rb/Sr vs. Sr/Ba plot (Fig. 5c), a negative

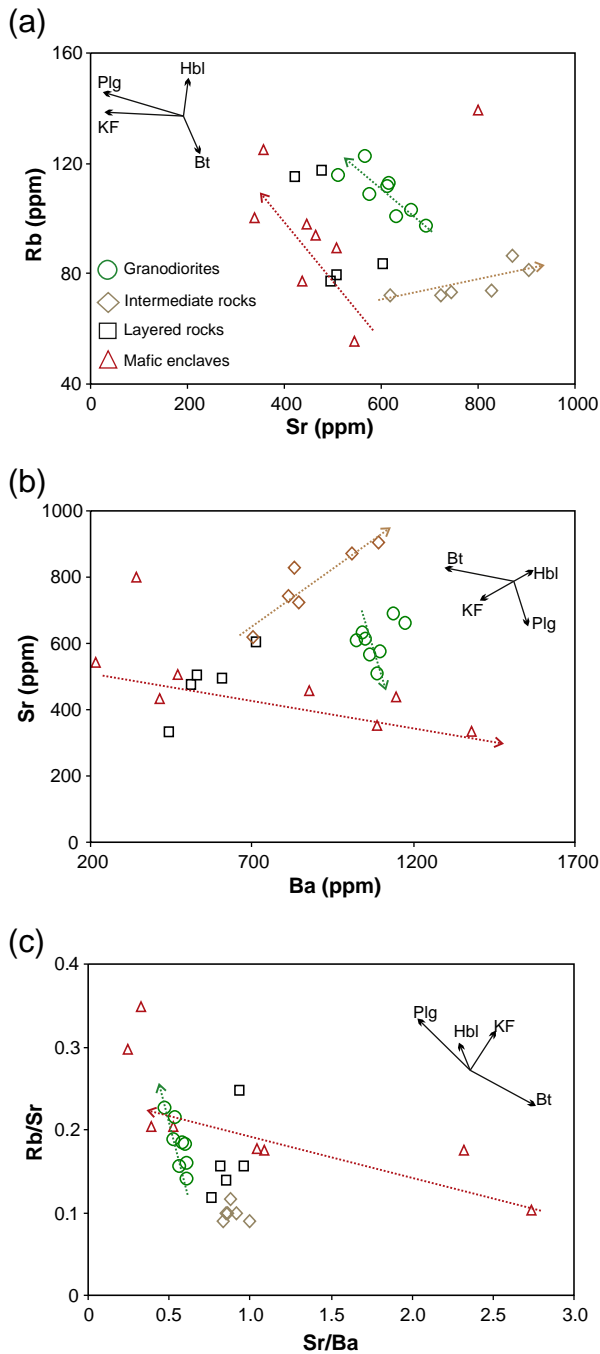


Fig. 5. (a) Rb vs. Sr; (b) Sr vs. Ba; (c) Rb/Sr vs. Sr/Ba plots for rocks from the Rio Maria suite (Bannach area). The vectors indicate the influence of fractionation of plagioclase (Plg), potassium feldspar (KF), hornblende (Hbl) and biotite (Bt) in the composition of the residual liquids. The arrows show possible trends during fractional crystallization into of granodiorites, intermediate rocks and mafic enclaves.

correlation between these ratios in the granodiorites is apparent, with an important increase in the Rb/Sr ratio parallel to increasing silica, whereas the Sr/Ba ratio remains almost constant. In the mafic enclaves, the correlation is also negative but, in this case, it is the Sr/Ba ratio that shows a larger variation. Finally, in the intermediate rocks, the Rb/Sr and Sr/Ba ratios do not show significant variations.

Granodiorites, intermediate rocks, and mafic enclaves display distinct geochemical trends in the Rb vs. Sr, Sr vs. Ba, and Rb/Sr vs. Sr/Ba plots (Fig. 5a, b, c). If we assume an evolution by fractional crystallization for each variety of rock, the trends shown by the granodiorites and mafic enclaves can be explained by simultaneous fractionation

of plagioclase and amphibole (Table 1; Fig. 5a, b). Moreover, the mentioned diagrams show that these two varieties derived from two entirely distinct liquids and the proportions of fractionated amphibole and plagioclase also differ. The trends defined by the intermediate rocks indicate fractionation of amphibole and biotite, reflected in the important increase of Sr and Ba and small variation in Rb along differentiation.

5.2.2. Sr and Y

The Sr and Y contents in the magmas are dependent of the composition of their sources (Moyen, 2009), but for similar sources the presence or absence of plagioclase or garnet between the fractionating phases during magma genesis and differentiation is also extremely relevant. Sr concentrations tend to be significantly lower in melts generated at relatively low pressures in the plagioclase domain of stability (Zamora, 2000; Martin et al., 2005). Y geochemical behavior is

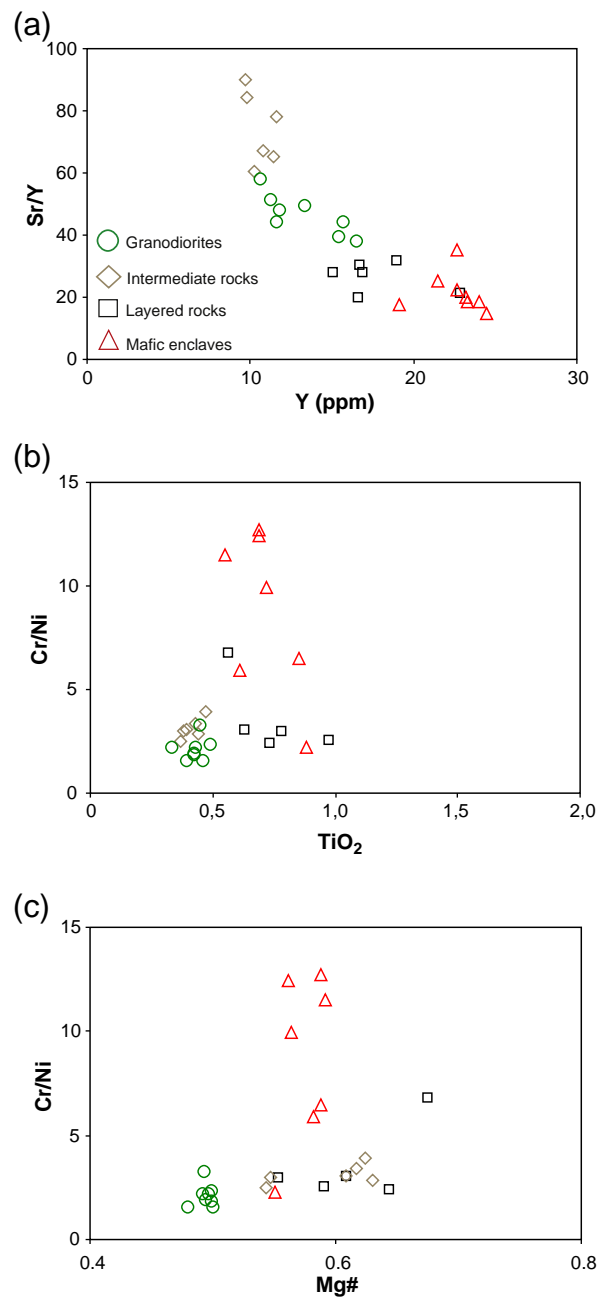


Fig. 6. (a) Sr/Y vs. Y; (b) Cr/Ni vs. TiO₂; (c) Cr/Ni vs. Mg# plots for rocks from the Rio Maria suite (Bannach area).

similar to that of Yb, and a low Y content in the melt is also generally seen as an indication of the presence of significant amounts of garnet in the residue. Consequently, the Sr/Y ratio behavior is similar to that of the La/Yb ratio during melting events that produce garnet and consume plagioclase (Moyen and Stevens, 2006). In addition, because of the strong influence of pressure conditions in plagioclase and garnet stability, for similar source compositions, Sr/Y ratios are a good pressure indicator.

The studied intermediate rocks have the highest Sr/Y ratios and the lowest Y contents (Table 1; Fig. 6a), the mafic enclaves show the highest Y contents and the lowest Sr/Y ratios values, and the values found in the granodiorite are in between those of intermediate rocks and mafic enclaves.

5.2.3. Cr and Ni

Mantle peridotites have a Cr/Ni ratio around 1.5 (Taylor and McLennan, 1985; McDonough and Sun, 1995) and its possible metasomatism by TTG melts would not significantly modify their Cr/Ni ratio because the $Cr_{\text{peridotite}}/Cr_{\text{TTG}}$ and $Ni_{\text{peridotite}}/Ni_{\text{TTG}}$ are very high (10 and 20, respectively). Consequently, the Cr/Ni ratio of the magmas derived from a metasomatized mantle is strongly dependent on the residual assemblage of mantle melting (Martin et al., 2005). Several possible residual phases of mantle melting have a $Kd_{(Cr/Ni)}^{\text{min/liq}}$ greater than one (orthopyroxene = 2.5; garnet = 4.4; pargasite = 4; Rollinson, 1993) but their effect could be buffered by olivine ($Kd_{(Cr/Ni)}^{\text{min/liq}} \sim 0.1$; Rollinson, 1993). The range of Cr/Ni ratios vary from 1.5 to 3.0 in the granodiorites and between 2.5 and 4 in the intermediate rocks. In the mafic enclaves Cr/Ni ratios attain their highest values (>5 and, generally, >10; Fig. 6b, c). These values point to differences in the residual assemblage of the mafic enclaves, in one hand, and intermediate rocks and granodiorites, in the other hand, and suggest the presence of mineral phases with $Kd_{(Cr/Ni)}^{\text{min/liq}} < 1$ (e.g. olivine) in the mafic enclaves magma residue and its probable absence or little influence in those of other varieties.

5.2.4. Rare earth elements

Granodiorites and intermediate rocks display similar patterns (Fig. 7) of rare earth elements (REE), with a pronounced enrichment in light rare earth elements (LREE) and strong to moderate fractionation of heavy rare earth elements (HREE) (La/Yb_N ratios of 15.52 to 44.38, granodiorites; 17.20 to 41.28, intermediate rocks), associated with a small or absent Eu anomaly (Eu/Eu* from 0.94 to 1.03, in both granodiorites and intermediate rocks; Table 1). The patterns of REE in the layered rocks and mafic enclaves show a less pronounced enrichment in LREE and a minor fractionation of HREE compared to granodiorite and intermediate rocks (La/Yb_N ratios of 6.57 to 11.32, enclaves; 11.92 to 14.37, layered rocks). This feature is associated with a small or absent (layered rocks; Eu/Eu* from 0.90 to 1.00) or

moderate negative europium anomaly (mafic enclaves; Eu/Eu* from 0.65 to 0.75).

The lack of a significant variation in the Eu/Eu* ratio from the intermediate rocks to the granodiorites is an evidence that these rocks were not linked by fractional crystallization process (Fig. 7) and that they could be derived from at least two distinct magmas, both with sanukitoid affinity, but originated from different degrees of melting of a modified mantle source (Oliveira et al., 2009).

Granodiorites and intermediate rocks show REE patterns with a concave shape of the HREE branch (Fig. 7), which suggests that amphibole was probably an important fractionating phase. This is not observed in the REE patterns of the layered rocks, and, along with the minor fractionation of HREE in those rocks compared with the granodiorites and intermediate rocks, it suggests that the process of amphibole accumulation determined the REE signature of these rocks (Oliveira et al., 2010). Besides their higher contents of HREE and important negative europium anomaly, the REE patterns of mafic enclaves display a convex shape of the LREE branch pattern. These aspects and the geochemical evidence shown above indicate that the mafic enclaves and the other varieties of rocks of the studied sanukitoid suite are not comagmatic and that, in the case of the former, plagioclase was a more important residual or fractionating phase than garnet during partial melting or fractional crystallization processes.

6. Geochemical modeling and petrogenesis

The geochemical data presented above demonstrate that the granodiorites, intermediate rocks, mafic enclaves, and layered rocks of the Bannach area all have sanukitoid characteristics in common. However, a preliminary evaluation of trace element data indicates that the three former varieties are cogenetic but not comagmatic rocks (this paper; cf. also Oliveira et al., 2009, 2010). Nevertheless, a possible relationship between these rocks by fractional crystallization was also evaluated by modeling. The hypothesis of a magmatic link between the layered rocks and granodiorites or intermediate rocks was also tested. Additionally, we evaluated whether or not different degrees of metasomatism of a mantle source or of assimilation of peridotite by slab-melts could explain the contrasting geochemical aspects of the studied rocks. Finally, the effect of variable degrees of partial melting of the source in the primitive magma composition was considered.

Thus, we have tested fractional crystallization, assimilation and partial melting models quantitatively in order to establish constraints for the petrogenesis of the Rio Maria sanukitoid suite. The nature of the magma source of these rocks, including the possible influence of processes of mantle metasomatism or assimilation of peridotite by slab-melts, was also investigated. This investigation was done using major elements, as well as selected trace elements, including REE.

6.1. Methodology of modeling

We performed mass balance calculations for the major elements using the program GENESIS (Teixeira, 2005). The model is calculated by adjusting the relative proportions of fractionating or residual minerals from the initial melt or source, respectively, to reproduce the composition of the expected melt. The quality of the model is evaluated using the sum of the squared residuals ($\sum R^2$), and the model is consistent if $\sum R^2 < 1$. For trace elements modeling, Excel tables created by Sergio C. Valente (Universidade Federal Rural do Rio de Janeiro, Brazil) were employed. The mineral/liquid partition coefficients (K_d) used in the modeling are available from Supplemental data Tables A3 and A4. Most of them are from Rollinson (1993).

The compositions of the initial liquids of the intermediate rocks, granodiorites and mafic enclaves are not precisely known and need to be estimated. In the case of intermediate rocks and granodiorites,

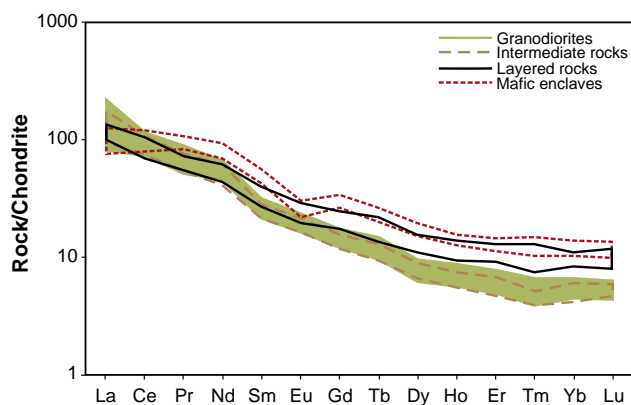


Fig. 7. Chondrite-normalized REE patterns for the rocks of the Rio Maria suite of Bannach area (normalization values from Evensen et al., 1978).

Table 2
Major elements compositions of minerals used for the major element modeling of crystallization and accumulation processes related to the rocks from Rio Maria suite (Bannach area).

Mineral	Layered rocks		Mafic enclaves		Intermediate rocks		Granodiorites	
	Amphibole	Biotite	Amphibole	Biotite	Amphibole	Biotite	Amphibole	Biotite
SiO ₂ (wt.%)	43.36	37.75	47.01	37.32	48.36	37.38	47.50	37.53
TiO ₂	1.59	1.12	1.06	1.16	0.47	0.39	0.92	1.03
Al ₂ O ₃	11.68	16.02	6.98	15.67	5.96	16.00	7.36	15.09
FeO	10.42	15.13	15.37	18.24	13.85	14.84	14.92	16.31
MnO	0.13	0.17	0.35	0.23	0.28	0.19	0.35	0.22
MgO	14.91	13.81	12.99	12.72	13.90	14.89	12.58	13.65
CaO	12.61	0.02	12.23	0.04	12.44	0.00	12.27	0.05
Na ₂ O	1.77	0.05	1.09	0.11	0.88	0.11	0.94	0.08
K ₂ O	0.84	9.88	0.74	9.52	0.47	9.32	0.68	9.49
Total	97.31	93.95	97.82	95.01	96.61	93.12	97.52	93.45

Data source: Oliveira et al. (2010). Total Fe reported as FeO.

although some comparisons with other samples have been made, the samples with the lowest silica contents of each group were used as representatives of the initial liquids (ADR-4A and MFR-114, respectively; Table 1). In the case of the mafic enclaves, the sample with the lowest silica content was not assumed as a representative, and the next sample in the range of silica was used (MD-02C; Table 1).

The compositions of the fractionating amphibole and biotite were taken from selected representative analyses (Oliveira et al., 2010) of these minerals found in intermediate rocks, granodiorites, mafic enclaves, and layered rocks of the Rio Maria suite (Table 2). The compositions of plagioclase, potassium feldspar, apatite and zircon are those corresponding to magmatic compositions found in Archean granitoids (Martin, 1985). In our partial melting and assimilation modeling, the compositions of the residual mineral phases tested include those given by Nixon et al. (1981), Rapp et al. (1999), and Moyen et al. (2001) (see more details below).

6.2. Fractional crystallization modeling

We have examined the following hypotheses: (1) whether the intermediate rocks and granodiorites could be related by fractional crystallization and, (2) if each group evolved internally by that process. Additionally, we have evaluated a possible magmatic link between the layered rocks and granodiorites or intermediate rocks through accumulation processes. A derivation of the intermediate rocks and granodiorite from the mafic enclave magma by fractional

crystallization was also tested but results were not acceptable ($\sum R^2 > 10$). A similar conclusion was also suggested by geochemical evidence and, for this reason, that hypothesis was discarded.

In the fractional crystallization modeling assuming that granodiorites derive from intermediate rocks, the sample ADR-4B (Table 1) was assumed as the parent and the sample MFR-114 (Table 1) as the daughter. The best models obtained were fractionating (1) amphibole + biotite, and (2) + plagioclase. However, even in these cases, the sums of the squared residuals are relatively high ($\sum R^2 > 2$, Table 3) and both fractionates give a bad fit for the REE (Fig. 8a, c). Other trace elements, especially Ba, Y, Nb, and Zr (Fig. 8b, d), decrease with fractionation, which is the opposite of increasing trend observed in the analyzed samples of intermediate rocks and granodiorite. Hence, for the derivation of the granodiorite magma from that of intermediate rocks, it is concluded that an acceptable model was not obtained. This observation reinforces the hypothesis that these rocks are not comagmatic.

To test if internal variation in the group of intermediate rocks was compatible with fractional crystallization, the sample ADR-4A was used as the parent and sample MFR-102 as the daughter. Two major element models fractionating amphibole + biotite ± apatite (Table 3) gave consistent results and were selected for trace element modeling. The lowest sums of the squared residuals ($\sum R^2 = 0.773$, model 1, Table 3) occur when apatite is also fractionated, and in this case, the fractionating phases, composed of 73% of amphibole, 22% of biotite, and 5% of apatite, represent 17% of the original liquid. For rare earth

Table 3
Modeling major element compositions and fractionated mineral assemblages for differentiation of the Rio Maria suite (Bannach area).

Varieties	Intermediate to granodiorite		Intermediate rocks			Granodiorites			Intermediate rock to layered rock				Granodiorite to layered rock		
	MFR-114	1	2	MFR-102	1	2	MFR-80A	1	2	MFR-12B	MFR-12A	Dark layer	Gray layer	Dark layer	Gray layer
SiO ₂ (wt.%)	62.52	62.78	62.80	62.15	61.98	61.69	66.49	66.48	66.37	52.60	53.41	50.40	51.87	52.49	53.32
TiO ₂	0.46	0.44	0.44	0.39	0.47	0.46	0.33	0.48	0.49	0.56	0.78	0.69	0.85	0.59	0.80
Al ₂ O ₃	15.23	15.29	15.27	14.5	14.98	15.05	14.55	14.53	14.62	10.91	14.76	11.97	14.97	11.20	14.79
Fe ₂ O ₃	5.10	4.70	4.72	5.73	5.16	4.91	3.74	4.05	4.11	9.90	9.44	8.9	9.03	9.81	9.40
MgO	2.61	3.63	3.64	4.11	4.08	3.83	1.85	1.61	1.65	10.51	5.98	12.5	7.24	10.61	5.99
CaO	4.40	3.79	3.77	4.65	5.00	5.27	3.02	2.89	2.65	9.30	7.88	12.1	9.78	9.22	7.98
Na ₂ O	4.30	4.57	4.56	4.21	4.42	4.45	4.13	4.43	4.41	2.06	2.99	1.20	2.00	1.90	2.79
K ₂ O	2.93	2.38	2.39	2.24	1.96	1.99	3.75	3.56	3.75	1.03	2.00	0.45	2.45	0.99	1.98
P ₂ O ₅	0.17	0.28	0.27	0.14	0.12	0.16	0.14	0.13	0.13	0.15	0.23	0.20	0.25	0.16	0.24
Plagioclase	–	–	2.40	–	–	–	–	54.40	55.40	–	–	–	10.27	–	10.27
Amphibole	–	89.10	87.30	–	73.20	67.26	–	38.40	44.60	–	–	100.00	89.73	100.00	89.73
Biotite	–	10.90	10.30	–	21.80	32.74	–	7.20	–	–	–	–	–	–	–
Apatite	–	–	–	–	5.00	–	–	–	–	–	–	–	–	–	–
$\sum R^2$	–	2.04	2.04	–	0.77	1.21	–	0.33	0.45	–	–	14.53	12.25	0.43	0.14
% Crystallization	–	15.00	15.00	–	17.00	19.00	–	25.00	25.00	–	–	–	–	–	–
% Accumulation	–	–	–	–	–	–	–	–	–	–	–	50.00	30.00	50.00	30.00

Total Fe reported as Fe₂O₃.

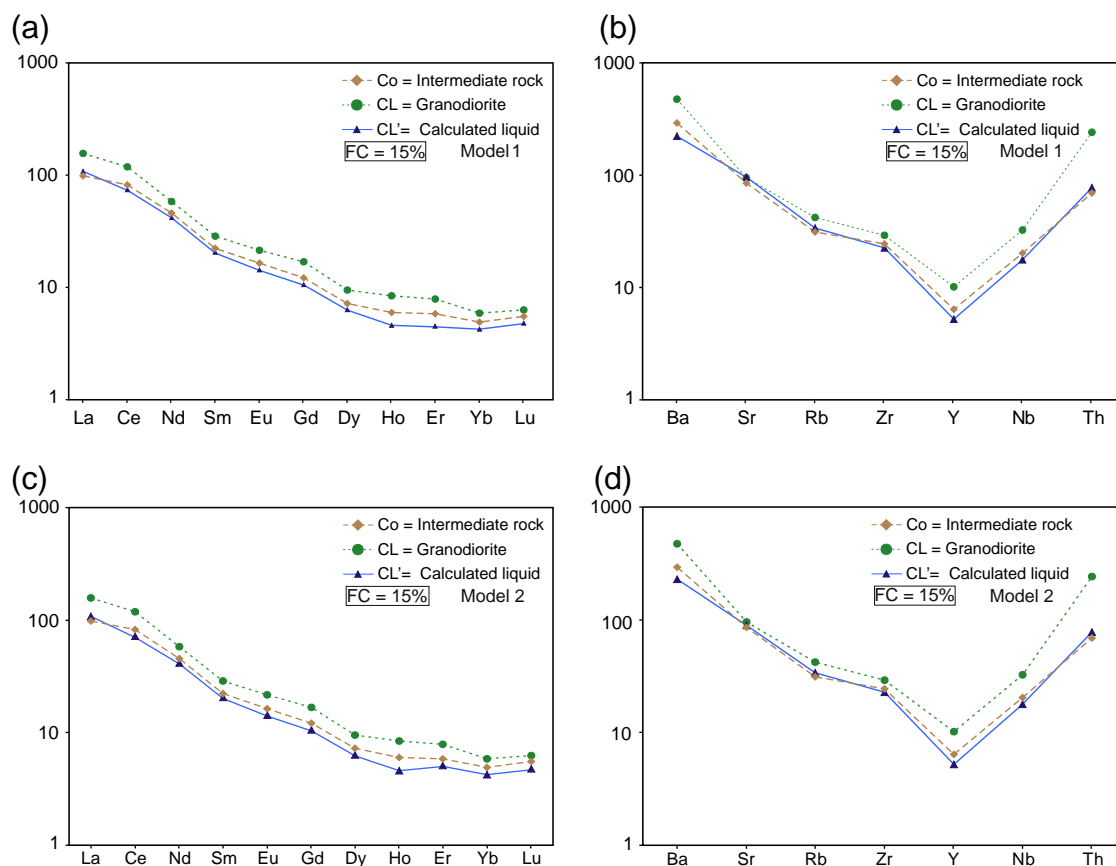


Fig. 8. Fractional crystallization (FC) modeling from the intermediate rocks (parent) to granodiorites (daughter). (a, c) REE patterns (normalization values from Evensen et al., 1978); (b, d) Trace elements plots; (a, b) model 1; (c, d) model 2; FC is percentage of crystallization.

elements and additional trace elements, in the two models the patterns (not shown) of the assumed parent magma, calculated liquid and intermediate rocks are superimposed and thus inconclusive.

In the case of granodiorites, the sample MFR-114 was used as the parent and MFR-80A as the daughter. Two major element models, both showing $\sum R^2 < 1$ and plagioclase and amphibole as the major fractionating phases (~55% and 38% to 45%, respectively; Table 3), were selected for trace element modeling. In one of these models, biotite was also included in the fractionating phases (7%; model 1, Table 3). In these models, the fractionating assemblages correspond to 25% of the original liquid, and both fractionates gave a good fit for the REE (Fig. 9a, c) and the other evaluated trace elements (Fig. 12b, d).

Assuming a cumulate origin for the layered rocks (Oliveira et al., 2010), we tested whether these rocks could be derived from the parental liquids of the granodiorites or intermediate rocks. For the granodiorites and intermediate rocks, the samples with the lowest silica contents were assumed as representatives of the initial liquid from which the layered rocks could have derived. We have examined whether the initial liquid was able to generate the dark (sample MFR-12B) and gray (sample MFR-12A) layers, which compose these rocks, by accumulation of amphibole, mainly. Assuming the intermediate composition as the initial liquid, trace element models give poor fits for REE and other trace elements between calculated liquid compositions and that of the layered rocks (Supplemental Fig. A2a, b, c, d). On the other hand, when we have tested the granodiorite magma as the initial liquid, in the major element models, best fits ($\sum R^2 < 1$, Table 3) were obtained with the composition of both, dark and gray layers. According to the major and trace element models, the accumulation of 30% and 50% of amphibole \pm plagioclase from the initial liquid would be able to generate the gray and dark layers, respectively

(Table 3). These models gave an excellent fit for REE and other trace elements (Fig. 10a, b, c, d).

Assuming a cumulate origin for the layered rocks (Oliveira et al., 2010), we tested whether these rocks could be derived from the parental liquids of the granodiorites or intermediate rocks. For the granodiorites and intermediate rocks, the samples with the lowest silica contents were assumed as representatives of the initial liquid from which the layered rocks could have derived. We have examined whether the initial liquid was able to generate the dark (sample MFR-12B) and gray (sample MFR-12A) layers, which compose these rocks, by accumulation of amphibole, mainly. Assuming the intermediate composition as the initial liquid, trace element models give poor fits for REE and other trace elements between calculated liquid compositions and that of the layered rocks (Supplemental Fig. A2a, b, c, d). On the other hand, when we have tested the granodiorite magma as the initial liquid, in the major element models, best fits ($\sum R^2 < 1$, Table 3) were obtained with the composition of both, dark and gray layers. According to the major and trace element models, the accumulation of 30% and 50% of amphibole \pm plagioclase from the initial liquid would be able to generate the gray and dark layers, respectively (Table 3). These models gave an excellent fit for REE and other trace elements (Fig. 10a, b, c, d).

6.3. Protoliths of the Rio Maria suite

The geochemical and isotopic characteristics of the Rio Maria suite suggest that both the mantle and subduction-related components must play an important role in the petrogenesis of these rocks (Oliveira et al., 2009). In addition, the P–T–H₂O–fO₂ estimate (Oliveira et al., 2010) points to oxidized and wet conditions for their precursor magmas,

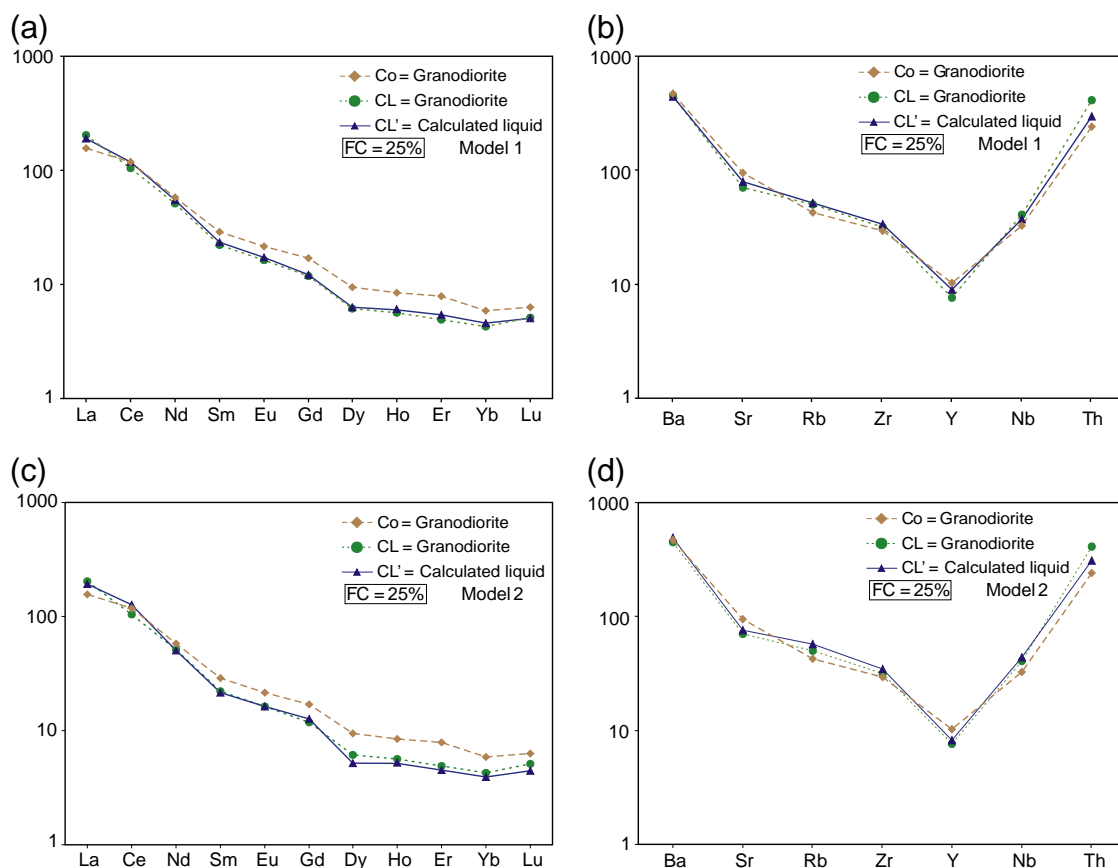


Fig. 9. Fractional crystallization (FC) modeling into of granodiorites. (a, c, e, g) REE patterns (normalization values from Evensen et al., 1978); (b, d, f, h) Trace elements plots; (a, b, c, d) Sample MFR-114 to sample MFR-27A, models 1 and 2; (e, f, g, h) Sample MFR-114 to MFR-80A, models 3 and 4; FC is percentage of crystallization.

which are two typical features of present-day arc magmas, including those with a strong slab melt signature, such as Pinatubo (Scaillet and Evans, 1999; Prouteau and Scaillet, 2003). The principal implication is that the characteristics of the Rio Maria Sanukitoid are compatible with a subduction zone geodynamic setting during the Archean in that area. In other Archean terranes containing high-Mg suites, a similar tectonic setting has also been proposed (Superior province, Stern and Hanson, 1991; Pilbara craton, Smithies and Champion, 2000; Karelian craton, Kovalenko et al., 2005; Halla, 2005; For an alternative model, see Bédard, 2006).

Two principal petrogenetic models involving a slab component have been proposed for the sanukitoid genesis. In the two-stage model, it is noted that sanukitoids are produced by the melting of a mantle source that has been extensively metasomatized by the assimilation of slab melts or fluids (Smithies and Champion, 2000; Kovalenko et al., 2005; Halla, 2005). In the single-stage model, it is proposed that a slab melt rising through peridotite mantle is able to assimilate olivine, which results in a “hybridized slab melt” with chemical composition similar to sanukitoids (Rapp et al., 1999, 2010). We have tested these possibilities using geochemical modeling and the results are presented and discussed below.

Rapp et al. (1999, 2010), Scaillet and Prouteau (2001) and Prouteau et al. (2001) have shown that the “effective” slab melt:peridotite ratio and the nature of the metasomatizing agent play an important role in the genesis of metasomatized mantle derived magmas. According to experiments performed by Rapp et al. (1999, 2010), that ratio could even determine the nature of the process. When the slab melt:peridotite ratio is approximately 3:1 to 2:1, the reaction product is a Mg-rich, high-SiO₂, hybridized melt. On the basis of experimental evidence, Rapp et al. (2010) demonstrate that this sanukitoid-like melt

will be in equilibrium with a garnet websterite or garnet orthopyroxene residue. However, when the slab melt:peridotite is nearly 1:1, the slab-derived TTG-like melt is fully consumed by metasomatic reactions that produce alkali-rich amphibole, pyrope-rich garnet, and both low-Mg# and high-Mg# orthopyroxene.

Prouteau et al. (2001) have also suggested that mantle metasomatism by slab melt is a more common and ten times more efficient process than metasomatism by hydrous fluids. Despite these restrictions, we have tested the hypothesis of origin of the Rio Maria sanukitoid magmas from the partial melting of a mantle source that was previously metasomatized by fluids derived from subducted sediments (Halla, 2005). Geochemical modeling showed that this kind of source for the Rio Maria sanukitoid magmas is unlikely. The obtained initial liquids have always lower silica contents compared to those of granodiorites and intermediate rocks and the fit for trace elements is unsatisfactory. Meantime, we cannot discard entirely a possible influence of subducted sediments in the genesis of Archean granitoid magmas of Rio Maria, even because Pb isotope data on these rocks are lacking (cf. Halla, 2005).

Anyway, the compositions of metasomatized mantle or hybridized slab melts able to originate the Rio Maria suite magmas are not precisely known, being necessary to estimate the compositions of the pristine slab-melt and peridotite mantle involved in the metasomatism or assimilation process. We tested two peridotite compositions representative of both depleted and primitive mantle, corresponding to harzburgite and spinel lherzolite, respectively, used by Rapp et al. (1999) in their experiments (their Table 7). The initial results of the modeling using depleted mantle compositions are not shown here, however the results indicated that the Ca and Al-poor, and Ni-rich harzburgite composition (Supplemental data Table A5) modified by

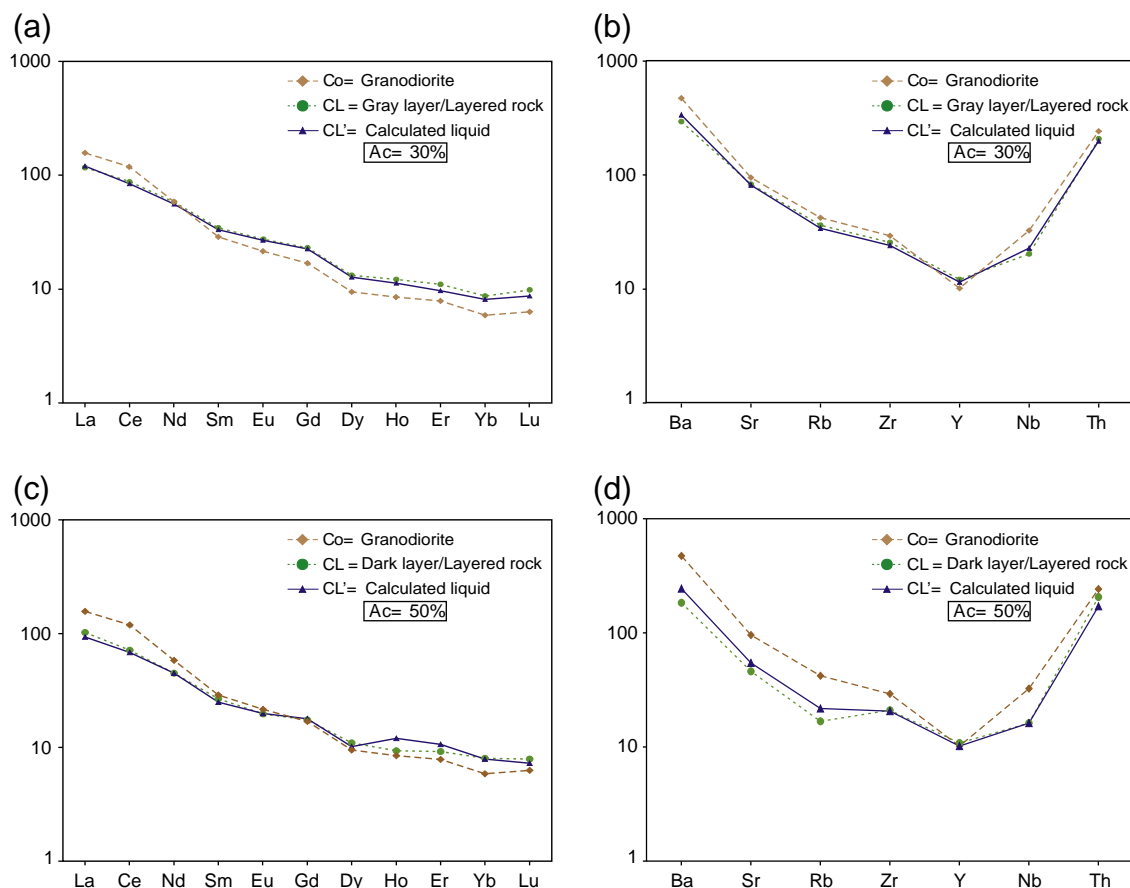


Fig. 10. Accumulation process (Ac) modeling of the layered rocks from granodiorite magma of the Rio Maria suite. (a, c) REE patterns (normalization values from Evensen et al., 1978); (b, d) Trace elements plots; (a, b) Gray layer, model 1; (c, d) Dark layer, model 2; Ac is percentage of accumulation.

metasomatism or assimilation processes is not able to generate the Rio Maria suite magmas. Thus, a primitive mantle composition corresponding to spinel lherzolite (Supplemental data Table A5) was used in the modeling.

Independent of the adopted model (single or two-stage), the magma source of the Rio Maria sanukitoid suite should apparently result from the interaction between a TTG slab-melt and a primitive mantle. For an effective interaction between the TTG melt and the mantle, a subduction tectonic setting is required. Partial melting experiments undertaken by Prouteau et al. (2001) and Scaillet and Prouteau (2001) demonstrated that slab hydrous metabasalts submitted at ca. 3.0 GPa pressures, in the garnet stability field, yield trondhjemitic melts, while dehydration melting at equivalent pressures of basalt underplated beneath the continental crust may yield silicic melts, but they will be granitic instead of trondhjemitic. This was explained by the fact that less water is available in the lower crust and dehydration melting reactions are favored. Based on these previous works, we have assumed that the slab-melts involved in the mantle assimilation or metasomatism had trondhjemitic instead of tonalitic compositions. Thus, in the geochemical modeling, we only tested representative trondhjemitic samples of the Mogno trondhjemite (~2.96 Ga; Almeida et al., 2011), Arco Verde tonalite (2.98–2.93 Ga; Macambira, 1992; Almeida et al., 2008) and Caracol tonalitic complex (2.95–2.93 Ga; Leite et al., 2004) of the Rio Maria granite–greenstone terrane as possible slab melt-derived TTG. The best fits were obtained using a sample of the Mogno trondhjemite (Supplemental data Table A5).

The modeling of different degrees of assimilation (5% to 40% of mantle component) of the peridotite mantle by slab melts (TTG; Mogno trondhjemite) gave a reasonable fit for 30% of harzburgitic

mantle, admitting a peritetic residue composed of garnet (18%), clinopyroxene (72%) and orthopyroxene (10%). The mass balance for Al₂O₃, CaO, MgO, and LREE was less satisfactory than for the other elements. On the other hand, the results of modeling of partial melting of the metasomatized mantle by slab melt were more consistent. Thus, both hypotheses corresponding to the one stage and the two stage model gave suitable fits according to the modeling. The first hypothesis has also been supported by experimental data (Rapp et al., 2010) and the second one by geochemical modeling (Smithies and Champion, 2000). However, geological and geochronological evidence to be discussed below indicate that in the Rio Maria terrane the two stage model is favored and, for this reason, it will be detailed in the following section.

6.3.1. Granodiorites

To test the hypothesis mentioned above, the granodiorite sample MFR-114, adopted as representative of the initial liquid of this rock type in previous modeling, was also assumed as the liquid resulting of the partial melting of the modified mantle source.

The metasomatized mantle source required to produce the granodiorite liquid by partial melting was obtained by mixing ~30% TTG into the spinel lherzolite mantle. The pertinent modified mantle whole rock composition is shown in Table 4. However, the compositions of the mineral phases that were present in this mantle at the time of melting are not known. Thus, different mineral compositions were tested: (1) those from peridotite xenoliths from South African kimberlites (Nixon et al., 1981); (2) those formed during metasomatic reactions between a slab melt and a peridotite (Rapp et al., 1999), and; (3) those from the incomplete metasomatic assemblage of Moyen et al. (2001).

Table 4

Chemical compositions of metasomatized mantle used in the protolith modeling of the rocks of Rio Maria suite.

Oxide	Metasomatized mantle		
	20% TTG-like melt	30% TTG-like melt	40% TTG-like melt
SiO ₂ (wt.%)	50.03	52.75	55.47
TiO ₂	0.17	0.17	0.18
Al ₂ O ₃	5.81	6.92	8.03
Fe ₂ O ₃	7.62	6.93	6.25
MnO	0.10	0.09	0.08
MgO	31.47	27.59	23.71
CaO	3.35	3.31	3.27
Na ₂ O	1.20	1.65	2.10
K ₂ O	0.27	0.40	0.53
P ₂ O ₅	0.02	0.03	0.04
Total	100.04	99.84	99.66
Ba (ppm)	120	178	236
Rb	12	17	23
Sr	143	208	274
Y	5	5	5
Zr	32	45	58
Nb	1	1	2
Th	2	3	3
Ni	1494	1308	1123
Cr	2470	2164	1858
La	5.45	8.14	10.84
Ce	9.95	14.72	19.49
Pr	1.19	1.73	2.27
Nd	4.48	6.32	8.16
Sm	0.78	0.97	1.17
Eu	0.23	0.27	0.31
Gd	0.87	0.98	1.08
Tb	0.14	0.15	0.15
Dy	0.89	0.91	0.92
Ho	0.18	0.17	0.17
Er	0.57	0.55	0.53
Tm	0.06	0.06	0.06
Yb	0.45	0.43	0.41
Lu	0.09	0.09	0.08

Incongruent melting modeling using mineral phases from Rapp et al. (1999) and with olivine and orthopyroxene in the residue gave inconsistent results ($\sum R^2 \geq 15$). Similar inconsistencies were obtained in calculations using the mineral compositions of Moyen et al. (2001) and the same mineral phases in the residual assemblage ($\sum R^2 \geq 17$). These results indicate that our assumed modified mantle with the mineral phase compositions used by Rapp et al. (1999) and Moyen et al. (2001) and olivine + orthopyroxene in the residue is probably not able to generate the initial liquids of the Rio Maria suite by partial melting processes. On the other hand, our mass balance calculations using the mineral phases of peridotite xenoliths from South African kimberlites and a residue without olivine gave excellent results ($\sum R^2 < 1$). The best fit model ($\sum R^2 = 0.646$, Table 5) was achieved with a proportion melt:residue ratio of 11% to 89%, the latter consisting of orthopyroxene (58%), garnet (28%), amphibole (11%), and clinopyroxene (3%). These same proportions of melt and residual mineral phases were tested in the trace elements modeling. The resulting model gave an excellent fit between the calculated initial liquid, which was generated from incongruent melting, and the assumed primitive granodiorite magma for REE and other trace elements (Fig. 11a, b).

Mass balance calculations including plagioclase as an additional residual phase also gave good fits for major elements ($\sum R^2 = 0.579$), but when compared with the assumed granodiorite primitive liquid, the trace element modeling indicated that this is a not acceptable model, because of the poor fit for REE and, especially, Ba and Sr.

6.3.2. Intermediate rocks

Based on the geochemical and petrographical data, Oliveira et al. (2009) suggested that intermediate rocks and granodiorites were generated from different degrees of melting of a similar source.

Thus, we have tested this hypothesis in mass balance calculations and trace element modeling. A metasomatized mantle source (~30% TTG melt into a spinel lherzolite mantle) and residual phases identical to those employed in the discussion of the origin of the granodiorite liquid were considered. The assumed primitive intermediate liquid should correspond in composition to the ADR-4A sample (Table 5).

An excellent fit ($\sum R^2 = 0.724$; Table 5) was obtained with a small increase in the melt proportion (14% melt, as compared to 11% in the case of the granodiorite liquid). In the residue, the proportions of orthopyroxene (60% vs. 58%) and garnet (28% vs. 26%) increased, and the proportions of clinopyroxene (2% vs. 3%) and amphibole (10% vs. 13%) decreased when compared to those observed in the case of the granodiorite liquid (Table 5). The REE pattern of the calculated primitive intermediate liquid (Fig. 13a) is consistent with the assumed intermediate magma composition, which is slightly more impoverished in HREE than the granodiorite one. This model also gave a good fit for the other trace elements considered (Fig. 12b).

6.3.3. Mafic enclaves

Despite their typical sanukitoid signature, the mafic enclaves show geochemical and petrographical peculiarities which should reflect differences in the origin of these rocks in relation to those of the granodiorite and intermediate rocks. To verify this premise, mass balance calculations involving the partial melting of a metasomatized mantle (with 30% of added TTG melt, which is identical to the case of granodiorite and intermediate rocks) to produce an initial liquid similar to the assumed mafic enclave composition (sample

Table 5

Mass-balance models for metasomatized mantle melting.

Oxide	Granodiorite (sample MFR-114)	Metasomatized mantle by 30% TTG-like melt	Proportions of melt and residual minerals
SiO ₂ (wt.%)	62.52	52.75	
TiO ₂	0.46	0.17	Clinopyroxene = 0.03
Al ₂ O ₃	15.23	6.92	Orthopyroxene = 0.58
Fe ₂ O ₃	5.10	6.93	Garnet = 0.26
MnO	0.07	0.09	Amphibole = 0.13
MgO	2.61	27.59	
CaO	4.40	3.31	Sum of the squared residuals = 0.646
Na ₂ O	4.30	1.65	
K ₂ O	2.93	0.40	
P ₂ O ₅	0.17	0.03	Melt fraction = 11%
Oxide	Intermediate rock (sample ADR-4A)	Metasomatized mantle by 30% TTG-like melt	Proportions of melt and residual minerals
SiO ₂ (wt.%)	58.47	52.75	
TiO ₂	0.47	0.17	Clinopyroxene = 0.02
Al ₂ O ₃	14.02	6.92	Orthopyroxene = 0.60
Fe ₂ O ₃	6.84	6.93	Garnet = 0.28
MnO	0.09	0.09	Amphibole = 0.10
MgO	5.81	27.59	
CaO	5.88	3.31	
Na ₂ O	3.77	1.65	Sum of the squared residuals = 0.724
K ₂ O	2.21	0.40	
P ₂ O ₅	0.17	0.03	Melt fraction = 14%
Oxide	Mafic enclave (sample MD-02C)	Metasomatized mantle by 20% TTG-like melt	Proportions of melt and residual minerals
SiO ₂ (wt.%)	51.38	50.03	
TiO ₂	0.72	0.17	Olivine = 0.38
Al ₂ O ₃	13.77	5.81	Orthopyroxene = 0.43
Fe ₂ O ₃	11.15	7.62	Plagioclase = 0.14
MnO	0.20	0.10	Amphibole = 0.05
MgO	7.38	31.47	
CaO	8.36	3.35	
Na ₂ O	3.53	1.20	Sum of the squared residuals = 0.024
K ₂ O	1.94	0.27	
P ₂ O ₅	0.37	0.02	Melt fraction = 9%

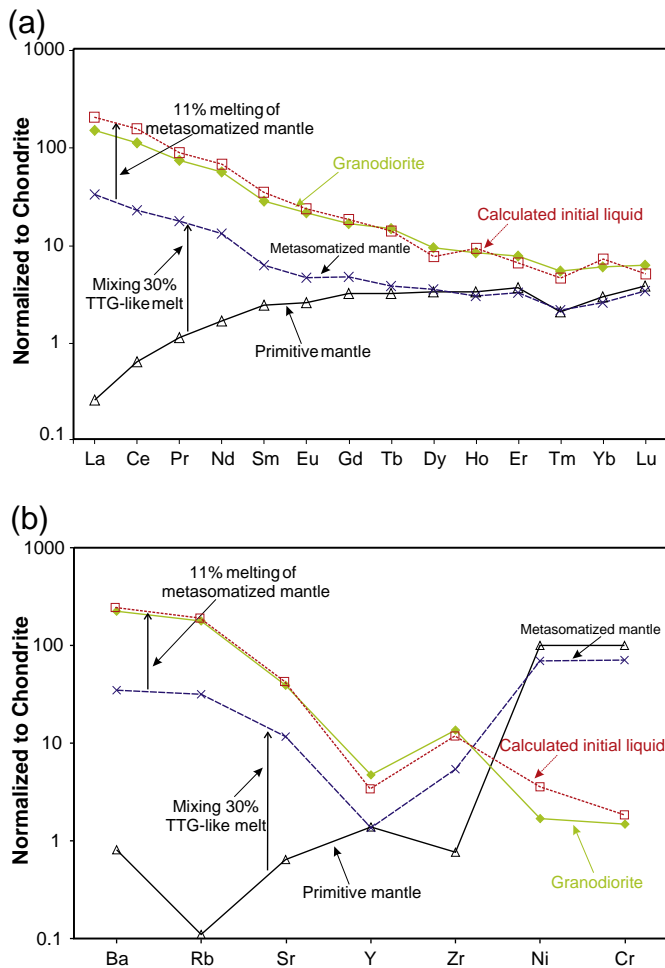


Fig. 11. (a) REE patterns (normalization values from Evensen et al., 1978); (b) Other trace elements. Comparison of the REE and other trace elements of the assumed primitive granodiorite magma composition with calculated liquids modeled by mixing 30% TTG melt in the peridotite mantle, following by 21% partial melting. The primitive and modified mantle compositions are shown in Electronic Supplemental datatable 5, 4 and 9. The melt proportions of metasomatized mantle suitable to generate intermediate magma and residual phase proportions are given in Table 5.

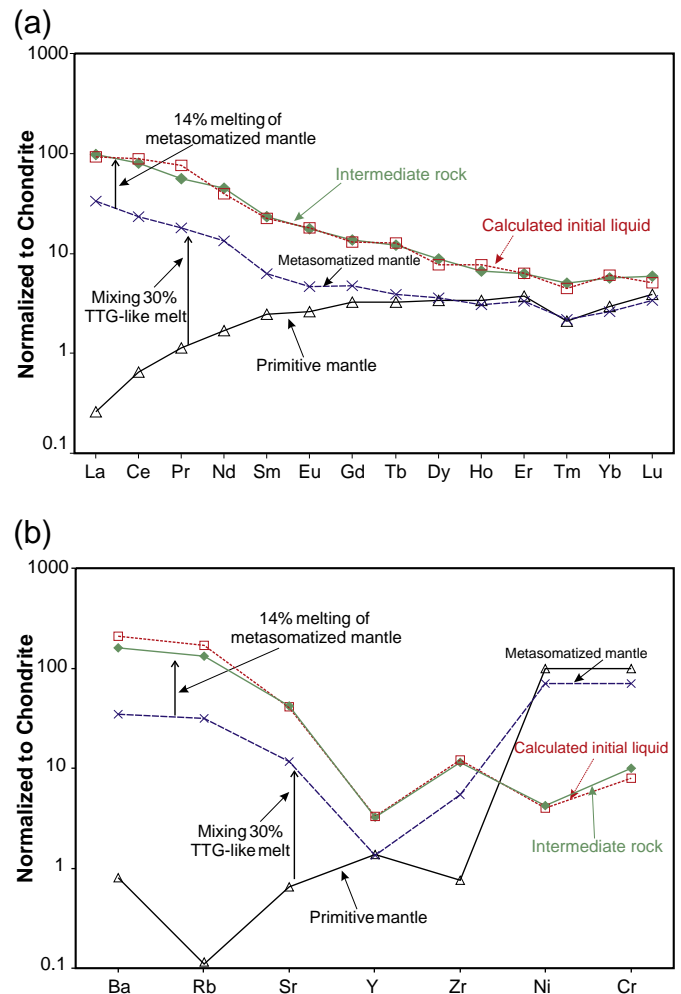


Fig. 12. (a) REE patterns (normalization values from Evensen et al., 1978); (b) Other trace elements. Comparison of the REE and other trace elements of the assumed primitive intermediate magma composition with calculated liquids modeled by mixing 30% TTG melt in the peridotite mantle, following by 24% partial melting. The primitive and modified mantle compositions are shown in Electronic Supplemental datatable 5, 4 and 9. The melt proportions of metasomatized mantle suitable to generate intermediate magma and residual phase proportions are given in Table 5.

MD-02C) were performed. The resulting model shows that for a proportion of 21% of melt and a residue comprised of olivine, orthopyroxene and plagioclase, a good fit was obtained for major elements ($\sum R^2 = 0.363$). However, for trace elements, and especially for the REE which are lower in the calculated liquid than in the mafic enclaves, the model gave a poor fit. Based on these results, we decided to examine the possibility of a different composition of the metasomatized mantle source.

Assuming a mantle that was modified by assimilation of 20% of TTG melt, major element modeling showed that 9% of partial melting of that mantle, leaving a residue comprised of olivine (38%), orthopyroxene (43%), amphibole (5%), and plagioclase (14%), was able to generate an initial liquid composition compatible with that of the assumed primitive mafic enclave liquid ($\sum R^2 = 0.024$). Mass balance calculations also indicated a good fit ($\sum R^2 = 0.074$) in the case of a model involving 11% of melting of the same source mentioned above, but without amphibole in the residual phase. For both models, trace element modeling gave good fits for REE and other trace elements. However, the model with amphibole as residual phase gave the best fit for the HREE, mainly Nd, Eu, Tb, and Ho, and was taken as representative of the melting process (Fig. 13a, b).

7. Discussion

7.1. Genesis of the Rio Maria sanukitoid magmas

The petrogenesis of the Rio Maria suite requires melting of a modified mantle source. Modeling suggests that the mantle source of the Rio Maria sanukitoid was extensively metasomatized by the addition of about 30% TTG-like melt to generate the granodiorite and intermediate magmas, and ~20% TTG-like melt in the case of mafic enclave magma. The partial melting processes that produced the granodiorite (11% of melt) and intermediate magma (14% of melt) left a residual assemblage formed by orthopyroxene, clinopyroxene, amphibole, and garnet. This is consistent with the experimental results obtained by Rapp et al. (2010), which indicate that liquids similar in composition to the Rio Maria granodiorite can be formed by partial melting of metasomatized mantle at high pressures.

In the case of the mafic enclave, the degree of melting was more limited (9%) and the residual assemblage showed relevant changes, plagioclase instead of garnet and presence of olivine. The first fact suggests that the magma of the mafic enclaves was originated at a lower pressure compared than that of the granodiorite and intermediate rocks. The lowest Sr/Y ratios, highest Y contents, and moderate

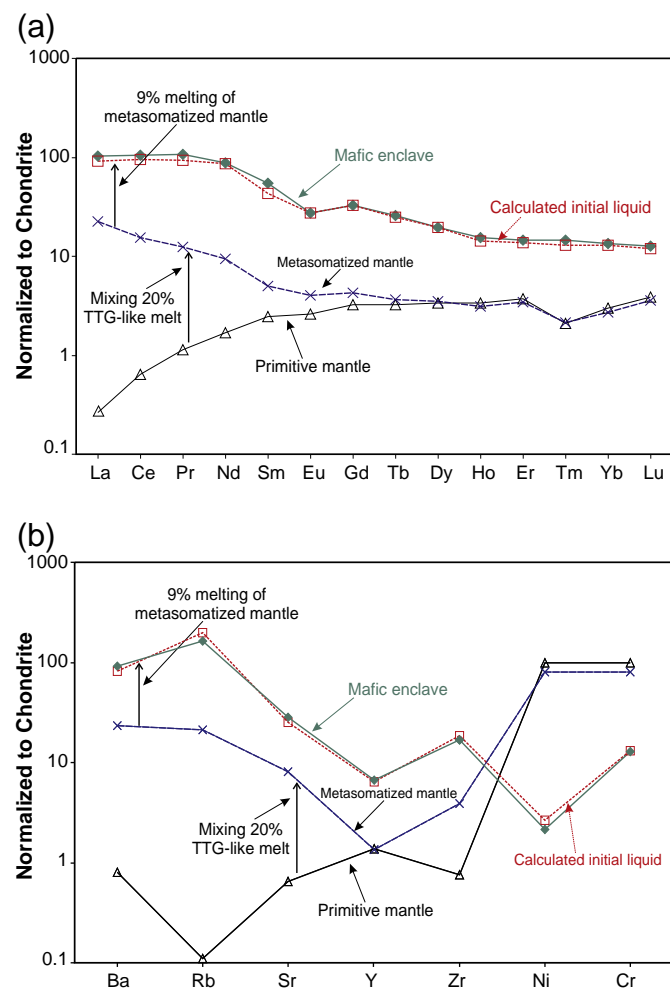


Fig. 13. (a) REE patterns (normalization values from Evensen et al., 1978); (b) Other trace elements. Comparison of the REE and other trace elements of the assumed primitive mafic enclave magma composition with calculated liquids modeled by mixing 20% TTG melt in the peridotite mantle, following by 9% partial melting. The primitive and modified mantle compositions are shown in Electronic Supplemental datatable 5, 4 and 9. The melt proportions of metasomatized mantle suitable to generate intermediate magma and residual phase proportions are given in Table 5.

negative Eu anomaly of the mafic enclaves are consistent with the presence of plagioclase as a residual phase and reinforce the results of the modeling. The presence of olivine in the residual phase is possibly reflected in the higher Cr/Ni ratios compared to granodiorites and intermediate rocks.

The adopted model implies the existence of an enriched mantle beneath the Rio Maria granite–greenstone terrane at approximately 2.87 Ga. The mantle enrichment could be caused by fluids liberated from a mantle plume (Jayananda et al., 2000) or from a subducted slab (Martin et al., 2005). However, our modeling suggests that a mantle modified by fluids will not have the adequate composition to generate the Rio Maria sanukitoid magmas. It also indicates, as the most likely hypothesis, that the Rio Maria mantle was previously enriched by TTG melts related to earlier subduction events (Shirey and Hanson, 1984; Stern et al., 1989; Stern and Hanson, 1991; Rapp et al., 1999; Smithies and Champion, 2000; Kovalenko et al., 2005).

The TTG series of Rio Maria were originally subdivided into older TTG series (2.98 to 2.92 Ga) and younger TTG series (~2.87 Ga) (Althoff et al., 2000; Leite et al., 2004; Dall'Agnol et al., 2006). However, recent geological and geochronological data (Guimarães et al., 2010; Almeida et al., 2011) have demonstrated that almost all TTG units were formed

in between 2.98 and 2.92 Ga (Arco Verde tonalite, Caracol tonalitic complex, Mogno trondhjemite, Mariázinha tonalite). The younger TTG units are, at present, limited to the Água Fria trondhjemite (ca. 2.86 Ga; Leite et al., 2004) exposed in a small area to the north of Xinguara (Fig. 1). The 2.87 Ga Rio Maria suite occurs in different areas of the Rio Maria terrane and, like sanukitoids elsewhere in the world (cf. Heilimo et al., 2011), its rocks are 110 to 50 Ma younger than those of the largely dominant TTG magmatism of that terrane (Leite et al., 2004; Almeida et al., 2011).

Althoff et al. (2000) and Souza et al. (2001) admitted a plate tectonic setting for the Rio Maria terrane in between 2.96 and 2.90 Ga. Leite et al. (2004) also suggested that its evolution at ca. 2.87 Ga was subduction-related. Our modeling results indicate that an active subduction tectonic setting was present in the terrane in between 2.98 and 2.92 Ga to explain the extensive formation of TTG magmas and the proposed metasomatism of the mantle by these magmas, before the melting process responsible for the origin of the sanukitoid magmas. In summary, the adopted model (cf. Almeida et al., 2011) implies: (1) an extensive generation of TTG magmas, at least in part derived from the partial melting of a mafic slab in a subduction setting; (2) the interaction of these TTG magmas with the mantle, resulting in a metasomatized mantle with a significant TTG component (20% to 30% in volume); (3) a tectonothermal event at ~2.87 Ga, which is possibly related to the slab-break-off that caused asthenosphere mantle upwelling, or to the action of a mantle plume, may have induced the melting of the metasomatized mantle and the generation of sanukitoid magmas; (4) the nature of the magmas depends of the degree of melting and on the depth (pressure) in which the melting process occurred; (5) the magmas ascended into the crust and evolved by fractional crystallization; (6) the magmas were emplaced at relatively shallow crustal levels, possibly forming laccoliths or sheet-like plutons (Souza et al., 1992).

Available Sm–Nd isotope data on the Rio Maria sanukitoid suite (Rämö et al., 2002) are limited to five samples (four granodiorites and one intermediate rock; Supplemental data Table A6). All samples gave ϵ_{Nd} ($t=2.87$ Ga) varying between 0.2 and 1.2 and T_{DM} model ages of 2923 to 3010 Ma, which suggests a juvenile character for the suite and the absence of an imprint of a preexistent crust. The coincidence between these T_{DM} model ages and the assumed crystallization ages of the Rio Maria older TTG suites can be seen as an additional evidence for a two stage process in the origin of the sanukitoid magmas in that region (cf. Kovalenko et al., 2005).

7.2. The role of pressure variation in the characteristics of sanukitoid series

The sanukitoid suites described in different Archean terranes consist of rocks that follow two distinct trends in modal Q–A–P diagrams. The dominant series varies from diorite and quartz diorite to the more abundant granodiorite and evolved along a granodioritic calc-alkaline trend (Fig. 3; Lameyre and Bowden, 1982). However, there is also an apparently subordinate series that is composed of monzodiorites, quartz monzodiorites, monzonites, and quartz monzonites, and follows a monzonitic trend (cf. Stern and Hanson, 1991, their Fig. 3). The latter series is represented in the Rio Maria terrane by the mafic enclaves (Fig. 3). Rocks representative of both series are commonly described in the Archean sanukitoid suites (Stern and Hanson, 1991; Smithies and Champion, 2000; Moyes et al., 2003; Halla, 2005; Lobach-Zhuchenko et al., 2005; Käpyaho, 2006; Heilimo et al., 2007), but a clear distinction between the mentioned series is commonly lacking. At least in the case of the Rio Maria suite as discussed above, the difference between both series is also evident in geochemical data. The observed differences suggest that these series cannot be derived from the same magma by fractional crystallization and are the result of the processes responsible for the origin of the magmas of each series. Our modeling indicated that the partial melting processes which generated the primitive magmas of the studied

rocks produced different residual assemblages. In the case of the granodiorite and intermediate rock magmas, garnet was a residual phase, whereas in the mafic enclave magma, garnet was absent and plagioclase was a residual phase. It was deduced that the mafic enclave magma was generated in the plagioclase stability domain and consequently at lower pressures, whereas the granodiorite and intermediate magmas were formed at comparatively higher pressures. This implies that the contrast in pressure in which the partial melting of the metasomatized mantle happened determines the differences in modal and geochemical composition between both granodioritic and monzonitic sanukitoid series.

To test our working hypothesis, we have selected chemical compositions of rocks which we have assumed as representative of both series from sanukitoid suites of different Archean terranes. Considering the fact that Sr, Y, and Sr/Y ratios are generally seen as good indicators of the pressure of melt formation (Defant and Drummond, 1990; Drummond and Defant, 1990), we decided to evaluate the geochemical behavior of the mentioned elements in classical sanukitoid suites and to establish comparisons with those of Rio Maria. In the Sr/Y vs. Y plot (Fig. 14), monzonites and quartz monzonites from the Karelian craton (Lobach-Zhuchenko et al., 2005) and monzonites from the Dharwar craton (Moyen et al., 2003) have low Sr/Y ratios and high Y contents, which are similar to those of the mafic enclaves of the Rio Maria suite. In contrast, granodiorites, quartz diorites, and diorites of different sanukitoid intrusions from eastern Finland (Arola suite, Käpyaho, 2006; Lieksa granodiorite, Halla, 2005; Kaapinsalmi tonalite, Heilimo et al., 2007) and the Pilbara craton (Smithies and Champion, 2000) have high to moderate Sr/Y ratios and low Y contents and are concentrated in the diagram in the same domain as the granodiorite and intermediate rocks of the Rio Maria suite (Fig. 14). This approach indicates that the contrasts observed between the granodioritic and monzonitic sanukitoid series are a general feature of these rocks. Our data also suggest that the origin of these series is strongly dependent on the pressure of the magma generation and, as a consequence, that the nature of the series could indicate the approximate depth of formation of its magma. If correct, this observation implies that the two fields shown in Fig. 14 are indicative not only of the nature of sanukitoid series but also of their pressure of formation. The field labeled A corresponds to rocks of the monzonitic series, which are supposed to be derived from relatively low pressure magmas and the field B includes rocks of the granodioritic series, which derived from magmas formed at higher pressures. For an

alternative hypothesis to explain the variation of the La/Yb and Sr/Y ratios see Moyen (2009).

7.3. The relationship between mafic enclaves and granodiorite magma

In all the occurrences of the Rio Maria suite, abundant and regularly distributed centimetric-sized mafic enclaves are systematically included in the host granodiorites (Oliveira et al., 2010). The modeling and geochemical data suggest that mafic and granodiorite magmas were originated at different depths and that the granodiorite magma was generated at a higher pressure than the mafic enclave magma. Field and petrographic aspects suggest a low viscosity contrast between enclaves and the Rio Maria granodiorite and indicated that the two magmas coexisted when both were still partly molten (Althoff et al., 2000; Leite, 2001; Oliveira et al., 2010). Thus, it was deduced that the granodiorite and mafic enclave magmas should mingled during their ascent and final emplacement. Only a limited interaction between both magmas should have occurred. This is indicated by field evidence and also by the relatively uniform geochemical behavior of each rock variety and the distinct trends displayed by their rocks in different modal and geochemical diagrams (Figs. 3, 4, and 5).

According to our modeling data, the sanukitoid granodiorite magma resulted from a partial melting of 11% of the metasomatized mantle at a pressure of >1000 MPa, whereas the enclave magma was generated at a pressure of ≤1000 MPa and resulted from a similar degree of partial melting (9%). It can be inferred that the enclave magma was at a higher lithospheric level and probably it should have lower volume compared to the granodiorite one. We can thus propose that the granodiorite magma ascended due to viscosity and gravity instabilities, attained the level of enclave magma formation, interacted with that magma, and ascended to the upper crust. The lower volume of the mafic magma caused its disruption in bubbles included and dispersed in the granodiorite magma. Both magmas were in a partially molten state and initiated their interaction. However, the relatively rapid ascent of the magmas prevented an intense re-equilibration and their essential primitive features were well preserved.

8. Summary and conclusions

The 2.87 Ga Rio Maria suite consists of Archean sanukitoid rocks of the Rio Maria granite–greenstone terrane and intrudes greenstone belts and TTG series. In the Bannach area, it is composed of four principal groups of rocks: granodiorites, intermediate rocks, layered rocks and mafic enclaves. Geochemical data demonstrated that these rocks have a sanukitoid signature and are not related by fractional crystallization.

Petrogenetic modeling, indicates that the internal evolution of intermediate magma was caused by the fractionation of amphibole + biotite ± apatite, whereas granodiorites evolved by the fractionation of plagioclase + amphibole ± biotite. Layered rocks have been derived from the granodiorite magma by an accumulation of 50% of amphibole, in the case of dark layer, and an accumulation 30% of amphibole ± plagioclase, in the case of the gray layer.

Geochemical data and modal compositions indicated that mafic enclaves (monzonitic series) and granodiorites or intermediate rocks (granodioritic series) follow two distinct trends in modal Q–A–P and geochemical diagrams and a link by fractional crystallization is not consistent. These two series are also found in other Archean cratons and their clear distinction is extremely relevant for the understanding of the origin and evolution of sanukitoid series.

According to modeling, the petrogenesis of the Rio Maria suite required the melting of a modified mantle source that was extensively metasomatized by the addition of about 30% TTG melt to generate the granodiorite (11% of melt) and intermediate magmas (14% of

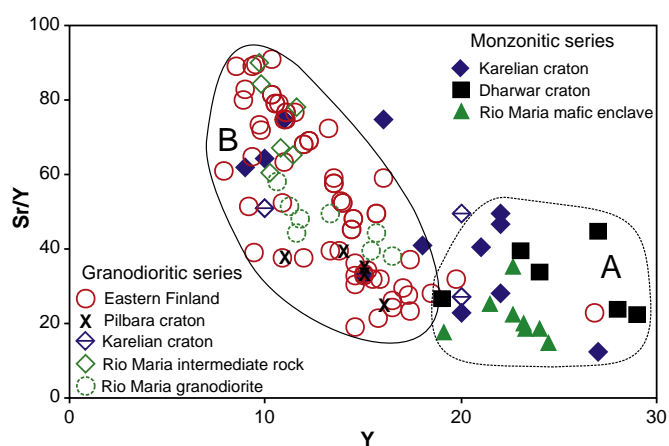


Fig. 14. Sr/Y vs. Y plot for rocks from the Rio Maria suite (Bannach area) and from sanukitoid suites of the Eastern Finland (Halla, 2005; Käpyaho, 2006; Heilimo et al., 2007), Karelian craton (Lobach-Zhuchenko et al., 2005) and Dharwar craton (Moyen et al., 2001, 2003). Fields A – monzonitic sanukitoid series, and B – granodioritic sanukitoid series.

melt) and ~20% TTG melt in the case of mafic enclave magma (9% of melt). In the case of the granodiorite and intermediate rock magmas, garnet was a residual phase, whereas in the mafic enclave magma, garnet was absent and plagioclase was a residual phase. The lowest Sr/Y ratios, highest Y contents, and moderately negative Eu anomaly of the mafic enclaves, are consistent with the presence of plagioclase as a residual phase and reinforce the results of modeling. This observation suggests that the contrast in pressure, in which it occurred the partial melting of the metasomatized mantle could be determinant in the differences in modal and geochemical composition between both the granodioritic (granodiorites and intermediate rocks) and monzonitic (mafic enclaves) sanukitoid series.

In summary, the adopted model for the generation of the rocks of the Rio Maria suite implies: (1) an extensive generation of TTG magmas, at least in part derived from the partial melting of a mafic slab in a subduction setting; (2) the interaction of these TTG magmas with the mantle, resulting in a metasomatized mantle with a significant TTG component (20% to 30% in volume); (3) a tectonothermal event at ~2.87 Ga, possibly related to the slab-break-off, causing asthenosphere mantle upwelling, or to the action of a mantle plume, may have induced the melting of the metasomatized mantle and the generation of sanukitoid magmas; (4) the nature of the magmas depends on the degree of melting and on the depth (pressure) in which the melting process occur; (5) the granodiorite magma ascended and mingled with the less voluminous mafic enclave magma; (6) the magmas ascended to the crust, evolved by fractional crystallization and were emplaced at relatively shallow crustal levels, possibly forming laccoliths or sheet-like plutons (Souza et al., 1992).

Supplemental data – Analytical methods were described by Gaudette et al. (1998): Isotopic ratios were measured in a FINNIGAN MAT 262 mass spectrometer and data were acquired in the dynamic mode using the ion-counting system of the instrument. For each step of evaporation, a step age is calculated from the average of the $^{207}\text{Pb}/^{206}\text{Pb}$ ratios. When different steps yield similar ages, all are included in the calculation of the crystal age. If distinct crystals furnish similar mean ages, then a mean age is calculated for the sample. Crystals or steps showing lower ages probably reflect Pb loss after crystallization and are not included in sample age calculation. Common Pb corrections were made according to Stacey and Kramers (1975) and only blocks with $^{206}\text{Pb}/^{204}\text{Pb}$ ratios higher than 2500 were used for age calculations. $^{207}\text{Pb}/^{206}\text{Pb}$ ratios were corrected for mass fractionation by a factor of 0.12% per a.m.u, given by repeated analysis of the NBS-982 standard, and analytical uncertainties are given at the 2σ level.

Supplementary materials related to this article can be found online at doi:10.1016/j.lithos.2011.08.017.

Acknowledgments

We would like to acknowledge O. T. Rämö, J. Halla, E. Heilimo, A. Heinonen, and M.I. Kurhila for guidance and assistance during field trip in the Eastern Finland terranes. We acknowledge S. Valente for help with our modeling. The detailed reviews by Jaana Halla and Jean-François Moyen and discussions with them and B. Scaillot, L. V. S. Nardi and V. A. Janasi were fully appreciated and greatly contributed to the improvement of the paper. M. A. Galarza Toro is acknowledged for help in Pb-evaporation on zircon dating (Para-Iso – UFPA). This research received financial support from CNPq (Roberto Dall'Agnol – Grants 476075/2003-3, 307469/2003-4; 484524/2007-0, PRONEX – Proc. 66.2103/1998; Marcelo Augusto de Oliveira – CNPq M.Sc. and Dr. scholarship; José de Arimatéia Costa de Almeida – CAPES and CNPq, respectively, M.Sc. and Dr. scholarship), and the Federal University of Pará (UFPA). This paper is a contribution to the Brazilian Institute of Amazonia Geosciences (INCT program – CNPq/MCT/FAPESPA – Proc. 573733/2008-2) and to the IGCP 599 project.

References

- Almeida, J.A.C., Oliveira, M.A., Dall'Agnol, R., Althoff, F.J., Borges, R.M.K., 2008. Relatório de Mapeamento Geológico na escala 1:100,000 da Folha Marajoara (SB-22-Z-C V). Programa GeoBrasil, CPRM – Serviço Geológico do Brasil. 147pp.
- Almeida, J.A.C., Dall'Agnol, R., Dias, S.B., Althoff, F.J., 2010. Origin of the Archean leucogranodiorite–granite suites: evidence from the Rio Maria. *Lithos* 120, 235–257.
- Almeida, J.A.C., Dall'Agnol, R., Oliveira, M.A., Macambira, M.J.B., Pimentel, M.M., Leite, A.A.S., 2011. Zircon geochronology and geochemistry of the TTG suites of the Rio Maria granite–greenstone terrane: implications for growth of Archean crust of Carajás Province, Brazil. *Precambrian Research* 187, 201–221.
- Althoff, F.J., Barbey, P., Boullier, A.M., 2000. 2.8–3.0 Ga plutonism and deformation in the SE Amazonian craton: the Archean granitoids of Marajoara (Carajás Mineral province, Brazil). *Precambrian Research* 104, 187–206.
- Barros, E.M., Sardinha, A.S., Barbosa, J.P.O., Krimski, R., Macambira, M.J.B., 2001. Pb–Pb and U–Pb zircon ages of Archean syntectonic granites of the Carajás Metallogenic Province, northern Brazil. *Simposio Sudamericano de Geologia Isotópica*, 3. Pucón, Chile. Sociedade Geológica de Chile. (CD ROM).
- Bédard, J.H., Brouillette, P., Madore, L., Berclaz, A., 2003. Archean cratonization and deformation in the northern Superior Province, Canada: an evaluation of plate tectonic versus vertical tectonic models. *Precambrian Research* 127, 61–87.
- Bédard, J.H., 2006. A catalytic delamination-driven model for coupled genesis of Archean crust and sub-continental lithospheric mantle. *Geochimica et Cosmochimica Acta* 70, 1188–1214.
- Condie, K.C., 2005. TTGs and adakites: are they both slab melts? *Lithos* 80, 33–44.
- Dall'Agnol, R., Rämö, O.T., Magalhães, M.S., Macambira, M.J.B., 1999. Petrology of the anorogenic, oxidised Jamon and Musa granites, Amazonian Craton: implications for the genesis of Proterozoic, A-type Granites. *Lithos* 46, 431–462.
- Dall'Agnol, R., Teixeira, N.P., Rämö, O.T., Moura, C.A.V., Macambira, M.J.B., Oliveira, D.C., 2005. Petrogenesis of the Paleoproterozoic rapakivi A-type granites of the Archean Carajás metallogenic province, Brazil. *Lithos* 80, 101–129.
- Dall'Agnol, R., Oliveira, M.A., Almeida, J.A.C., Althoff, F.J., Leite, A.A.S., Oliveira, D.C., Barros, C.E.M., 2006. Archean and Paleoproterozoic granitoids of the Carajás metallogenic province, eastern Amazonian craton. In: Dall'Agnol, R., Rosa-Costa, L.T., Klein, E.L. (Eds.), *Symposium on Magmatism, Crustal Evolution, and Metallogenesis of the Amazonian Craton. Abstracts Volume and Field Trips Guide*. Belém, PRONEX-UFPA/SBG-NO, pp. 99–150.
- Dall'Agnol, R., Almeida, J.A.C., Oliveira, M.A., Leite, A.A.S., Althoff, F.J., 2011. The Mesoproterozoic Rio Maria granite greenstone terrane, Eastern Amazonian Craton, Brazil: granitoid magmatism and geologic evolution. *International Symposium on Precambrian Accretionary Orogens*, Delhi, India.
- Defant, M.J., Drummond, M.S., 1990. Derivation of some modern arc magmas by melting of young subducted lithosphere. *Nature* 347, 662–665.
- Drummond, M.S., Defant, M.J., 1990. A model for trondhjemite–tonalite–dacite genesis and crustal growth via slab melting: Archean to modern comparisons. *Journal of Geophysical Research* 95, 21503–21521.
- Evans, O.C., Hanson, G.N., 1997. Late- to post-kinematic Archean granitoids of the S.W. Superior Province: derivation through direct mantle melting. In: de Wit, M.J., Ashwal, L.D. (Eds.), *Greenstone Belts*. Oxford University Press, Oxford, pp. 280–295.
- Evensen, N.M., Hamilton, P.T., O'Nions, R.K., 1978. Rare earth abundances in chondritic meteorites. *Geochimica et Cosmochimica Acta* 39, 55–64.
- Gaudette, H.E., Lafon, J.M., Macambira, M.J.B., Moura, C.A.V., Scheller, T., 1998. Comparison of single filament Pb evaporation/ionization zircon ages with conventional U–Pb results: examples from the Precambrian of Brazil. *Journal of South American Earth Science* 11, 351–363.
- Guimarães, F.V.G., Dall'Agnol, R., Almeida, J.A.C., Oliveira, M.A., 2010. Caracterização geológica, petrográfica e geoquímica do trondhjemito Mogno e tonalito Maria-zinha, Terreno granito–greenstone de Rio Maria, Pará. *Revista Brasileira de Geociências* 40, 196–211.
- Guimarães, F.V., Dall'Agnol, R., Oliveira, M.A., Almeida, J.A.C., in press. *Geologia, Petrografia e Geoquímica do Quartzó-diorito Parazônia e Granodiorito Grotão, Terreno Granito–Greenstone de Rio Maria–Pará*. *Revista Brasileira de Geociências*.
- Halla, J., 2005. Late Archean high-Mg granitoids (sanukitoids) in the southern Karelian domain, eastern Finland: Pb and Nd isotopic constraints on crust–mantle interactions. *Lithos* 79, 161–178.
- Hanson, G.N., 1978. The application of trace elements to the petrogenesis of igneous rocks of granitic composition. *Earth Planetary Sciences Letters* 38, 26–43.
- Hanson, G.N., 1989. An approach to trace element modeling using a simple igneous system as an example. In: Lipin, B.R., McKay, G.A. (Eds.), *Geochemistry and mineralogy of rare earth elements*. *Reviews in Mineralogy* 21, 79–97.
- Heilimo, E., Mikkola, P., Halla, J., 2007. Age and petrology of the Kaapinsalmi sanukitoid intrusion in Suomussalmi, Eastern Finland. *Bulletin of the Geological Society of Finland* 79, 117–125.
- Heilimo, E., Halla, J., Hölttä, P., 2010. Discrimination and origin of the sanukitoid series: geochemical constraints from the Neoproterozoic western Karelian Province (Finland). *Lithos* 115, 27–39.
- Heilimo, E., Halla, J., Huhma, H., 2011. Single-grain zircon U–Pb age constraints of the western and eastern sanukitoid zones in the Finnish part of the Karelian Province. *Lithos* 121, 87–99.
- Huhn, S.R.B., Santos, A.B.S., Amaral, A.F., Ledsham, E.J., Gouveia, J.L., Martins, L.B.P., Montalvão, R.M.G., Costa, V.G., 1988. O terreno granito–greenstone da região de Rio Maria, Sul do Pará. *Congresso Brasileiro de Geologia*, 35, Belém. *Anais do congresso Brasileiro de Geologia*, Belém, pp. 1438–1453. SBG 3.
- Irvine, T.N., Baragar, W.R.A., 1971. A guide to the chemical classification of the common volcanic rocks. *Canadian Journal of Earth Sciences* 8, 523–547.

- Jayananda, M., Moyen, J.-F., Martin, H., Peucat, J.-J., Aury, B., Mahabaleswar, B., 2000. Late Archaean (2550–2520 Ma) juvenile magmatism in the Eastern Darwar craton, southern India: constraints from geochronology, Nd-Sr isotopes and whole rock geochemistry. *Precambrian Research* 99, 225–254.
- Käpyaho, A., 2006. Whole-rock geochemistry of some tonalite and high Mg/Fe gabbro, diorite, and granodiorite plutons (sanukitoid suite) in the Kuhmo district, Eastern Finland. *Bulletin of the Geological Society of Finland* 78, 121–141.
- Kober, B., 1986. Whole-grain evaporation for $^{207}\text{Pb}/^{206}\text{Pb}$ -age-investigations on single zircons using a double-filament source. *Contributions to Mineralogy and Petrology* 93, 482–490.
- Kovalenko, A.V., Clemens, J.D., Savatenkov, V.M., 2005. Petrogenetic constraints for the genesis of Archaean sanukitoid suites: geochemistry and isotopic evidence from Karelia, Baltic Shield. *Lithos* 79, 147–160.
- Lafon, J.M., Rodrigues, E., Duarte, K.D., 1994. Le granite Mata Surrão: un magmatisme monzogranitique contemporain des associations tonalitiques–trondhjemitiques–granodioritiques archéennes de la région de Rio Maria (Amazonie Orientale, Brésil). *Comptes Rendues de la Academie de Sciences de Paris*, t. 318 (serie II), 642–649 (In French).
- Lameyre, J., Bowden, P., 1982. Plutonic rock type series: discrimination of various granitoid series and related rocks. *Journal of Volcanology and Geothermal Research* 14, 169–186.
- Le Bas, M.J., Le Maitre, R.W., Streckeisen, A., Zanettin, B., 1986. A classification of volcanic rocks based on the total alkali–silica diagram. *Journal of Petrology* 27, 745–750.
- Le Maitre, R.W., 2002. A Classification of Igneous Rocks and Glossary of Terms. 2nd Edition. London, 193 pp.
- Leite, A.A.S., 2001. Geoquímica, petrogênese e evolução estrutural dos granitóides arqueanos da região de Xinguara, SE do Cráton Amazônico. Belém, Universidade Federal do Pará, Centro de Geociências. Doctor Thesis. Programa de Pós-Graduação em Geologia e Geoquímica, Centro de Geociências, UFPA (in Portuguese). 330p.
- Leite, A.A.S., Dall'agnol, R., Macambira, M.J.B., Althoff, F.J., 2004. Geologia e geocronologia dos granitóides arqueanos da região de Xinguara (PA) e suas implicações na evolução do Terreno Granito–Greenstone de Rio Maria. *Revista Brasileira de Geociências* 34, 447–458.
- Lobach-Zhuchenko, S.B., Rollinson, H., Chekulav, V.P., Arestova, N.A., Kovalenko, A.V., Ivanikov, V.V., Guseva, N.S., Sergeev, S.A., Matukov, D.I., Jarvis, K.E., 2005. The Archaean sanukitoid series of the Baltic shield—geological setting, geochemical characteristics and implications for their origin. *Lithos* 79, 107–128.
- Macambira, M.J.B., 1992. Chronologie U/Pb, Rb/Sr, K/Ar et croissance de la croûte continentale dans l'Amazonie du sud-est; exemple de la région de Rio Maria, Province de Carajás, Brésil. Doctor Thesis. Montpellier, Université Montpellier II-France. 212 pp. (In French).
- Macambira, M.J.B., Lafon, J.M., 1995. Geocronologia da Província Mineral de Carajás; Síntese dos dados e novos desafios. *Boletim do Museu Paraense Emílio Goeldi, série Ciências da Terra* 7, 263–287 (In portuguese).
- Macambira, M.J.B., Lancelot, J., 1996. Time constraints for the formation of the Archaean Rio Maria crust, southeastern Amazonian Craton, Brazil. *International Geology Review* 38, 1134–1142.
- Machado, N., Lindenmayer, Z.G., Krogh, T.E., Lindenmayer, D., 1991. U–Pb geochronology of Archaean magmatism and basement reactivation in the Carajás area, Amazon shield, Brazil. *Precambrian Research* 49, 329–354.
- Martin, H., 1985. Nature, origine et evolution d'un segment de croûte continentale archéenne: contraintes chimiques et isotopiques. Exemple de la Finlande orientale. *Mem.CAESS no. 1*. Rennes, France. 324 pp.
- Martin, H., 1994. The Archaean grey gneisses and the genesis of continental crust. In: *Condie, K.C. (Ed.), Archaean Crustal Evolution*. Elsevier, Amsterdam pp, pp. 205–259.
- Martin, H., 1999. The adakitic magmas: modern analogues of Archaean granitoids. *Lithos* 46 (3), 411–429.
- Martin, H., Smithies, R.H., Rapp, R., Moyen, J.-F., Champion, D., 2005. An overview of adakite, tonalite–trondhjemite–granodiorite (TTG), and sanukitoid: relationships and some implications for crustal evolution. *Lithos* 79, 1–24.
- McDonough, W.F., Sun, S.-S., 1995. Composition of the Earth. *Chemical Geology* 120, 223–253.
- Medeiros, H., 1987. Petrologia da porção leste do maciço Granodiorítico Rio Maria, Sudeste do Pará. 166p. M.Sc. Thesis. Programa de Pós-Graduação em Geologia e Geoquímica, Centro de Geociências, UFPA (in Portuguese).
- Moyen, J.-F., Martin, H., Jayananda, M., 2001. Multi-element geochemical modelling of crust–mantle interactions during late-Archaean crustal growth: the Closepet granite (South India). *Precambrian Research* 112, 87–105.
- Moyen, J.-F., Martin, H., Jayananda, M., Auvray, B., 2003. Late-Archaean granites: a typology based on the Dharwar Craton (India). *Precambrian Research* 2375, 1–21.
- Moyen, J.-F., Stevens, G., 2006. Experimental constraints on TTG petrogenesis: implications for Archaean geodynamics. In: *Benn, K., Mareschal, J.-C., Condie, K.C. (Eds.), Archaean Geodynamics and Environments*. Geophysical Monograph 164. American Geophysical Union, Washington, DC.
- Moyen, J.-F., 2009. High Sr/Y and La/Yb ratios: the meaning of the “adakitic signature”. *Lithos* 112, 556–574.
- Moyen, J.-F., 2011. The composite Archaean grey gneisses: petrological significance, and evidence for a non-unique tectonic setting for Archaean crustal growth. *Lithos* 123, 21–36.
- Nixon, P.H., Rogers, N.W., Gibson, I.L., Grey, A., 1981. Depleted and fertile mantle xenoliths from Southern African kimberlites. *Annual Review Earth Planetary Science* 9, 285–309.
- Oliveira, M.A., 2005. Geologia, Petrografia e Geoquímica do Granodiorito Sanukitóide Arqueano Rio Maria e Rochas Máficas Associadas, Leste de Bannach-PA. Universidade Federal do Pará. 141p. M.Sc. Thesis. Programa de Pós-Graduação em Geologia e Geoquímica, Centro de Geociências, UFPA (in Portuguese).
- Oliveira, M.A., Dall'Agnol, R., Althoff, F.J., 2006. Petrografia e Geoquímica do Granodiorito Rio Maria da região de Bannach e comparações com as demais ocorrências no terreno Granito–Greenstone de Rio Maria-Pará. *Revista Brasileira de Geociências* 36 (2), 313–326 (in Portuguese).
- Oliveira, M.A., Dall'Agnol, R., Althoff, F.J., Leite, A.A.S., 2009. Mesoarchean sanukitoid rocks of the Rio Maria Granite–Greenstone Terrane, Amazonian craton, Brazil. *Journal of South American Earth Sciences* 27, 146–160.
- Oliveira, M.A., Dall'Agnol, R., Scaillet, B., 2010. Petrological constraints on crystallization conditions of MesoArchaean Sanukitoid Rocks, southeastern Amazonian craton, Brazil. *Journal of Petrology* 51, 2121–2148.
- Prouteau, G., Scaillet, B., Pichavant, M., Maury, R.C., 2001. Evidence of mantle metasomatism by hydrous silicic melts derived from subducted oceanic crust. *Nature* 410, 197–200.
- Prouteau, G., Scaillet, B., 2003. Experimental constraints on the origin of the 1991 Pinatubo dacite. *Journal of Petrology* 44, 2203–2241.
- Rämö, O.T., Dall'Agnol, R., Macambira, M.J.B., Leite, A.A.S., de Oliveira, D.C., 2002. 1.88 Ga oxidized A-type granites of the Rio Maria region, eastern Amazonian craton, Brazil: positively anorogenic! *Journal of Geology* 110, 603–610.
- Rämö, O.T., 1991. Petrogenesis of the Proterozoic rapakivi granites and related basic rocks of southeastern Fennoscandia: Nd and Pb isotopic and general geochemical constraints. *Geological Survey Finland Bulletin* 355 161 pp.
- Rapp, R.P., Shimizu, N., Norman, M.D., Applegate, G.S., 1999. Reaction between slab-derived melts and peridotite in the mantle wedge: experimental constraints at 3.8 GPa. *Chemical Geology* 160, 335–356.
- Rapp, R., Yaxley, G., Norman, M.D., Shimizu, N., 2007. Comprehensive trace element characteristics of experimental TTG and sanukitoid melts. Sixth International Hut-ton Conference on the Origin of Granitic Rocks. Stellenbosch, South Africa.
- Rapp, R.P., Norman, M.D., Laporte, D., Yaxley, G.M., Martin, H., Foley, S.F., 2010. Continent formation in the Archaean and chemical evolution of the cratonic lithosphere: melt–rock reaction experiments at 3–4 GPa and petrogenesis of Archaean Mg-diorites (sanukitoids). *Journal of Petrology* 51, 1237–1266.
- Ringwood, A.E., 1975. Composition and Petrology of the Earth's Mantle. MacGraw-Hill Editor. 618 pp.
- Rollinson, H., 1993. Using Geochemical Data. Longman, London. 352 pp.
- Scaillet, B., Evans, B.W., 1999. The June 15, 1991, eruption of Mount Pinatubo: I. Phase equilibria and pre-eruption P–T–fO₂–fH₂O conditions of the dacite magma. *Journal of Petrology* 40, 381–411.
- Scaillet, B., Prouteau, G., 2001. Oceanic slab melting and mantle metasomatism. *Science Progress* 84 (4), 335–354.
- Shirey, S.B., Hanson, G.N., 1984. Mantle-derived Archaean monzodiorites and trachyandesites. *Nature* 310, 222–224.
- Smithies, R.H., Champion, D.C., Sun, S.-S., 2004. Evidence for early LREE-enriched mantle source regions: diverse magmas from the c. 3.0 Ga Mallina Basin, Pilbara Craton, NW Australia. *Journal of Petrology* 45 (8), 1515–1537.
- Smithies, R.H., Champion, D.C., 2000. The Archaean high-Mg diorite suite: links to tonalite–trondhjemite–granodiorite magmatism and implications for early Archaean crustal growth. *Journal of Petrology* 41 (12), 1653–1671.
- Souza, Z.S., Luiz, J.G., Cruz, J.C.R., Paiva, R.N., 1992. Geometria de greenstone belts arqueanos da região de Rio Maria (Sudeste do Pará, Brasil), a partir de interpretação gravimétrica. *Revista Brasileira de Geociências* 22 (2), 198–203.
- Souza, Z.S., Potrel, H., Lafon, J.M., Althoff, F.J., Pimentel, M.M., Dall'agnol, R., Oliveira, C.G., 2001. Nd, Pb and Sr isotopes of the Identidade belt, Na Archaean greenstone belt of the Rio Maria region (Carajás province, Brazil): implications for the Archaean geodynamic evolution of the Amazonian craton. *Precambrian research* 109, 293–315.
- Stacey, J.S., Kramers, J.D., 1975. Approximation of terrestrial lead isotope evolution by a two-stage model. *Earth and Planetary Science Letters* 26, 207–221.
- Stern, R.A., Hanson, G.N., Shirey, S.B., 1989. Petrogenesis of mantle-derived, LILE-enriched Archaean monzodiorites and trachyandesites (sanukitoids) in southwestern Superior Province. *Canadian Journal of Earth Sciences* 26, 1688–1712.
- Stern, A.L., Hanson, G., 1991. Archaean high-Mg granodiorite: a derivative of light rare earth element-enriched monzodiorite of mantle origin. *Journal of Petrology* 32, 201–238.
- Taylor, S.R., McLennan, S.M., 1985. The Continental Crust: Its Composition and Evolution. Blackwell Scientific, Oxford. 321 pp.
- Teixeira, L.R., 2005. GENESIS 4.0 – Software de Modelamento Geoquímico.
- Wilson, M., 1989. Igneous Petrogenesis. Academic Press, London. 466 pp.
- Zamora, D., 2000. Fusion de la croûte océanique subduite: approche expérimentale et géochimique. Université Thesis Université Blaise Pascal, Clermont-Ferrand, 314 pp.